THE SYNTHESIS OF BETA ALUMINA POWDERS

A thesis submitted to the UNIVERSITY OF CAPE TOWN
in fulfilment of the requirements for the degree of
DOCTOR OF PHILOSOPHY

by

ARNOLD VAN ZYL B.Sc. (Chem. Eng.) M.Sc. Pr.Eng.

AUGUST 1987

ACKNOWLEDGEMENTS

I would like to thank the following people for their contribution to this thesis:

- CSIR colleagues Stewart Hart, Mike Thackeray, Graham Duncan, Adele Forman and May Dorling
- Hamish Duncan and Peter Barrow from Beta Research and Development, Derby, UK
- Oelof Heckroodt from the University of Cape Town
- Angus Kingon from the North Carolina State University, USA
- Roger Wedlake from Anglo American Corporation, Johannesburg

ABSTRACT

THE SYNTHESIS OF BETA ALUMINA POWDERS

Arnold van Zyl (NIMR/CSIR, PO Box 395, PRETORIA 0001)

AUGUST 1987

Beta alumina solid electrolyte material is conventionally synthesized by the high temperature solid state reaction of α-Al_2O_3 with soda and a stabilizer ion such as lithia or magnesia. This reaction requires a reconstructive transformation of the α-Al_2O_3 oxygen sublattice and results in a two-phase mixture of β- and β"-Al_2O_3.

In order to maximize the preferred β"-Al_2O_3 phase an additional peak heat treatment schedule is required. This work investigated the replacement of the α-Al_2O_3 component of the reaction mixture with a range of synthetic aluminium hydroxide precursor materials.

Four different aluminium hydroxide precursors were synthesized by the controlled hydrolysis of a common aluminium isopropoxide parent material. The oxygen sublattice of each aluminium hydroxide precursor was engineered by varying the alkoxide hydrolysis conditions. These precursors were used to synthesize beta alumina powders by the high temperature solid state reaction with soda and lithia, resulting in powders with a nominal composition of $Li_{0.38}Na_{1.65}Al_{10.66}O_{17}$.

The solid state reactions were monitored by differential thermal analysis and thermogravimetric analysis. The structural development of the reaction products with increasing temperature, was monitored by powder X-ray diffraction.

A significant observation was the direct formation of single phase β"-Al_2O_3 at 1200 ^{o}C by the solid state reaction of soda and lithia with certain aluminium hydroxides. The work concludes with the proposal of a generalized mechanism relating the aluminium hydroxide precursor oxygen sublattice to the nature of the beta alumina reaction product.

TABLE OF CONTENTS

Page

CHAPTER 1

1.1 Introduction 1

1.2 Structure of Beta Alumina 4

1.3 Phase Relationships 11

1.4 The Fabrication of Beta Tubes 14

CHAPTER 2

2.1 Introduction 17

2.2 Classification of Aluminium Hydroxides 18

2.2.1 Amorphous alumina 19

2.2.2 Aluminium oxide hydroxides 21

2.2.2.1 Boehmite 21

2.2.2.2 Diaspore 23

2.2.3 Aluminium trihydroxides 23

2.2.3.1 Gibbsite 23

2.2.3.2 Bayerite 24

2.2.3.3 Nordstrandite 25

2.3 Phase Relationships in the Alumina-Water System 26

2.4 Thermal Dehydroxylation and Subsequent Reordering of Aluminium Hydroxides 28

2.5 Beta Alumina Crystallization Pathway 32

CHAPTER 3

3.1 Synthesis of High Purity Aluminium Hydroxide Materials 35

3.2 Raw Material Characterization 37

3.2.1 Monohydrates 39

3.2.2 Trihydrates 43

TABLE OF CONTENTS (Cont.)

Page

CHAPTER 4

4.1 Experimental Methods 52
4.1.1 Powder Preparation 53
4.1.2 Solid state reaction and characterization of precursor powders 54
4.2 Results 56
4.2.1 α-Al_2O_3 56
4.2.2 Hydrothermal boehmite 58
4.2.3 Pseudoboehmite 62
4.2.4 Bayerite 65
4.2.5 Gibbsite 68
4.3 Discussion 73
4.3.1 Two-phase β/β''-Al_2O_3 mixtures 73
4.3.2 Pure β''-Al_2O_3 formation 73
4.3.3 Intergrown β/β''-Al_2O_3 polytypes 78
4.4 Conclusions 80

CHAPTER 5

CONCLUSIONS AND FUTURE RESEARCH AREAS 81

REFERENCES 83

CHAPTER 1:

1.1 INTRODUCTION

This chapter serves as an introduction to the beta alumina solid electrolyte and reviews the application, crystal structure, phase relationships, and fabrication techniques of the material.

Beta alumina is a critical component of the ZEBRA high energy density battery system [Coetzer (1986)]. The ZEBRA battery consists of a positive electrode which comprises a transition metal such as iron or nickel in combination with molten $NaAlCl_4$ salt. The anode consists of molten sodium and is separated from the cathode by a β''-Al_2O_3 solid electrolyte. A typical cell configuration of the ZEBRA cell can be written as follows:

$$Na//\beta''Al_2O_3//NaAlCl_4//FeCl_2.Fe$$

A simplified cell reaction can be written as:

$$\underset{\text{charged}}{2Na + FeCl_2} \rightleftharpoons \underset{\text{discharged}}{2NaCl + Fe}$$

The $FeCl_2$ electrochemically active material is insoluble in the $NaAlCl_4$ molten salt and remains associated with the electronically conductive matrix. This configuration implies two distinct sodium ion conducting phases namely $NaAlCl_4$ and β''-Al_2O_3.

At an operating temperature of 250 ^{o}C the cell has an open circuit voltage of 2.35 and a theoretical energy density of more than 700 W/kg. A cross-section of a typical ZEBRA cell is presented in Fig. 1.1.

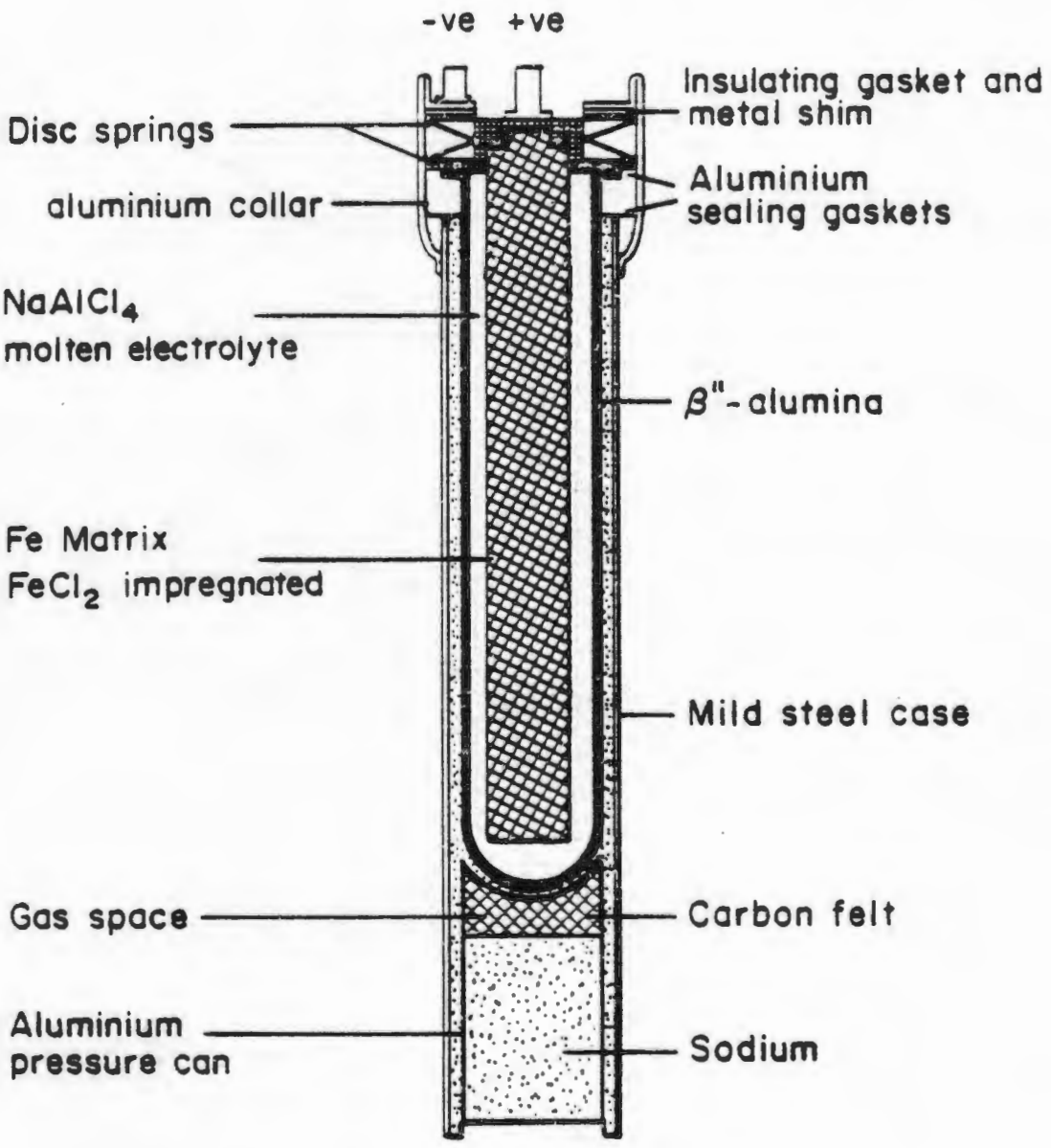

FIGURE 1.1: A cross-section of a typical ZEBRA cell

The polycrystalline, ceramic β''-Al_2O_3 solid sodium ion conductor is the focal point of much research and development.

In addition to having a high sodium ion conductivity at the operating temperature of 250 °C, the solid electrolyte must have the following properties:

- high electronic resistivity (insulating)
- toughness and mechanical integrity
- near theoretical density (above 3.16 g/cm^3)
- chemical resistance to sodium and the cathode materials.

Rankin and Merwin (1916) assigned the prefix beta to a material which they considered to be a high temperature modification of alumina. This form of alumina was always associated with high temperature treated alumina containing high levels of alkali or alkaline earth materials.

Later investigations by Bragg et al. (1931) and Beevers and Brohult (1936) showed that sodium oxide was necessary for the formation of beta alumina. This pioneering X-ray crystallographic work proposed the stoichiometry of the beta alumina to be $Na_2O.11Al_2O_3$. Peters et al. (1971) subsequently demonstrated that beta alumina with this stoichiometry is metastable, and is always soda-rich, corresponding more closely to a composition, $Na_2O.xAl_2O_3$ with x varying between 8 and 9.

Although the observed non-stoichiometry could often be ascribed to the presence of related phases in a single crystallite as reported by Bevan et al (1974), a deviation for ideal stoichiometry has been observed in single phase beta alumina, indicating an inherent tendency towards non-stoichiometry.

The most common form of beta alumina contains sodium as a cation. Scholder and Marsman (1963) have reported aluminates containing cations such as Ca^{2+}, Ba^{2+}, Sr^{2+}, Cs^{+}, Rb^{+}, K^{+} and

Ag^+. This has led to the foreign cation being incorporated in the name of the material, such as sodium beta alumina or silver beta alumina.

Throughout the subsequent text the two major crystallographic forms of sodium beta alumina will be referred to as β-Al_2O_3 and β''-Al_2O_3.

1.2 STRUCTURE OF BETA ALUMINA

A discussion of the structures of the two beta alumina phases will draw largely on the work of Mosely (1985). The beta alumina group of oxides consists of structures composed of slabs of four close-packed oxygen layers interspersed by layers with a low atom density which contain the mobile sodium (or other) cations. The close-packed oxide slabs accommodate Al^{3+} ions in both octahedral and tetrahedral interstices.

There are two main subgroups of beta alumina which differ in the stacking sequence of layers up the unique axis. The first subgroup (β-Al_2O_3) which is stacked according to a two-fold screw axis, contains a mirror plane through the layers of mobile cations and results in hexagonal crystal symmetry. The idealized structure of the unit cell of β-Al_2O_3 is shown in perspective in Fig. 1.2. Figure 1.3 shows a $11\bar{2}0$ section through the structure highlighting the oxygen stacking along the c-axis. The figure shows how the slabs of close-packed oxide extend normally to the hexagonal c-axis with adjacent slabs held apart by rigid Al-O-Al spacer units. Ionic diffusion occurs exclusively within the open planes perpendicular to the c-axis.

The β''-Al_2O_3 subgroup is stacked according to the three-fold screw axis, contains no mirror plane and has rhombohedral

symmetry. The idealized structure of the unit cell of β''-Al_2O_3 is shown in perspective in Fig. 1.2. The unit cell is 50% larger than that of β-Al_2O_3 by virtue of the difference in stacking sequence, as shown in Fig. 1.3. Adjacent close-packed oxide slabs are held apart by Al-O-Al spacer units, but in this structure alternate sodium atoms sites lie above and below the plane through the centre of the oxide spacer atoms and the Na^+ ion diffusion path encompasses a finite volume (the conduction slab) rather than a plane as in the β-Al_2O_3 structure. Structural parameters for β- and β''-Al_2O_3 are given in Tables 1.1 and 1.2.

The beta aluminas are known to be non-stoichiometric compounds. The conduction layers for β-Al_2O_3 and β''-Al_2O_3 are shown in Fig. 1.4 and indicate possible sites for excess sodium ion accommodation in the conduction plane. Peters et al. (1971) has shown that charge compensation for excess sodium can occur by aluminium vacancies in the spinel layers or by oxygen interstitial sites in the conduction plane. A neutron study by Roth (1976) revealed the presence of a displaced aluminium ion which binds with an interstitial oxygen ion in one of the mid-oxygen sites in the conduction plane resulting in a complex linear defect. The insertion of such an oxygen ion would allow two extra sodium ions into the conduction plane. Potential energy calculations by Wang (1975) appear to support the interstition oxygen bound to the displaced aluminium ion as the most energetically favourable charge compensation mechanism.

The high proportion of defect sites for the sodium ions in the conduction layers, as well as the open structure of the conduction plane imparts the beta aluminas with the ability to conduct sodium ions while remaining electronically insulating. This property of the material makes it an ideal solid electrolyte for high temperature batteries. Theoretical aspects of the conduction mechanisms in beta aluminas have been reported in detail by Manan (1976) and Highe (1981).

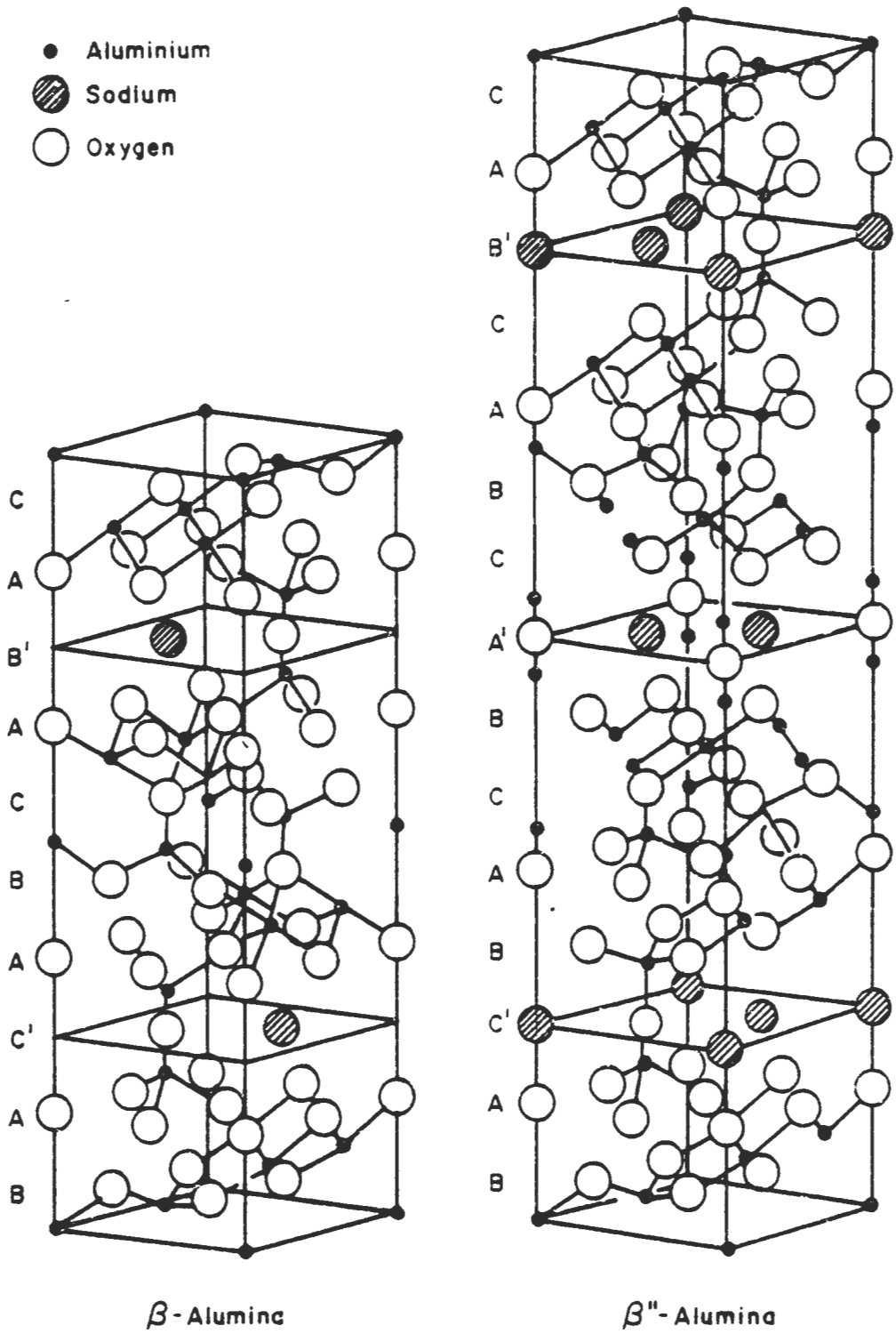

FIGURE 1.2: Perspective drawing of the idealized structures of β-Al_2O_3 and β"-Al_2O_3 (from Mosely 1985)

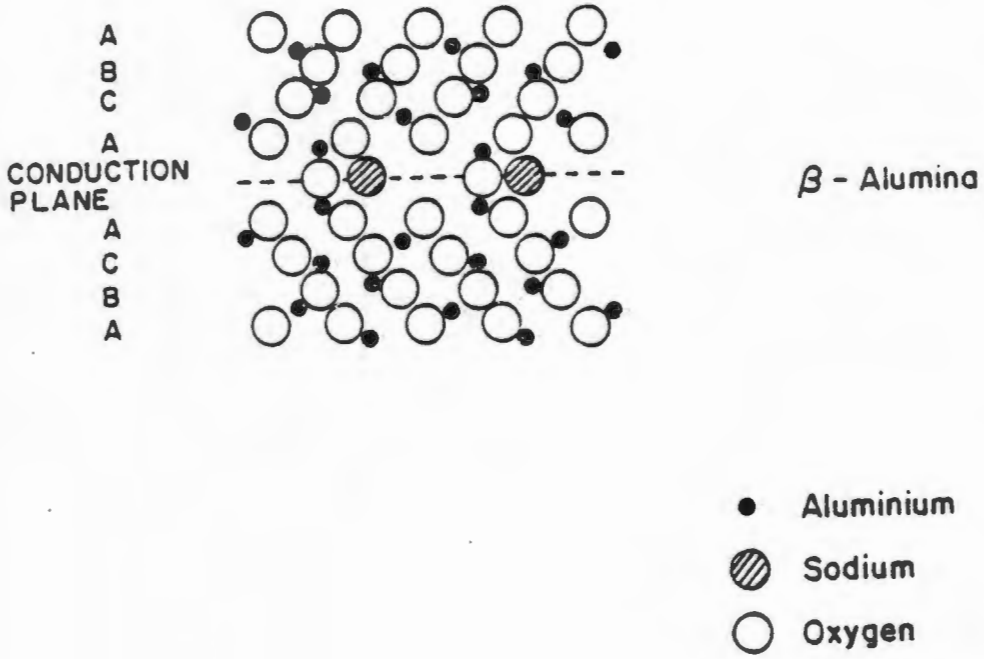

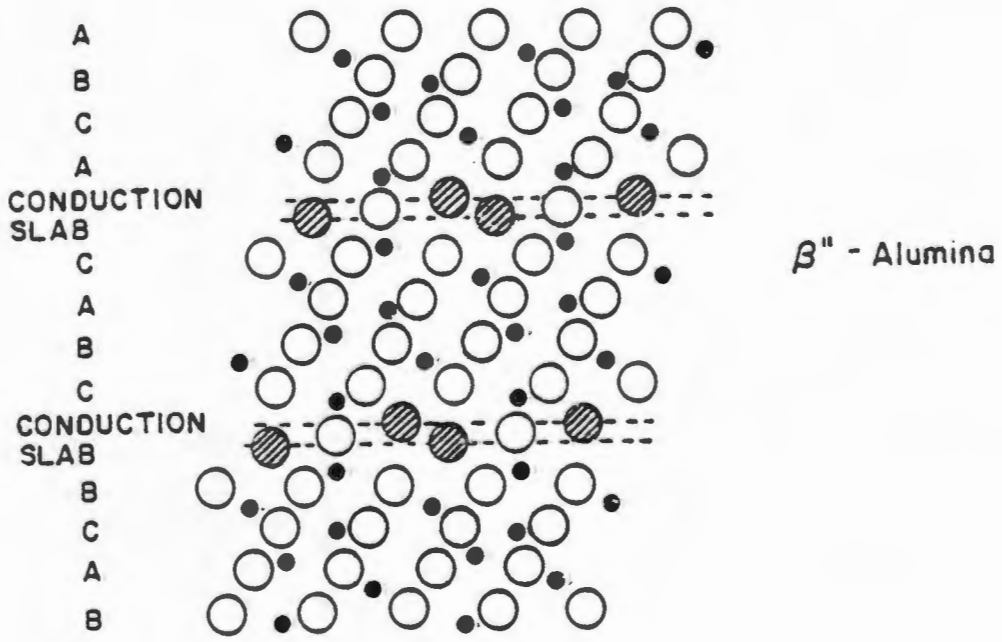

FIGURE 1.3: $11\bar{2}0$ section through the idealized structure of β-Al_2O_3 and β"-Al_2O_3 showing the stacking sequence along the c-axis (after Mosely 1985)

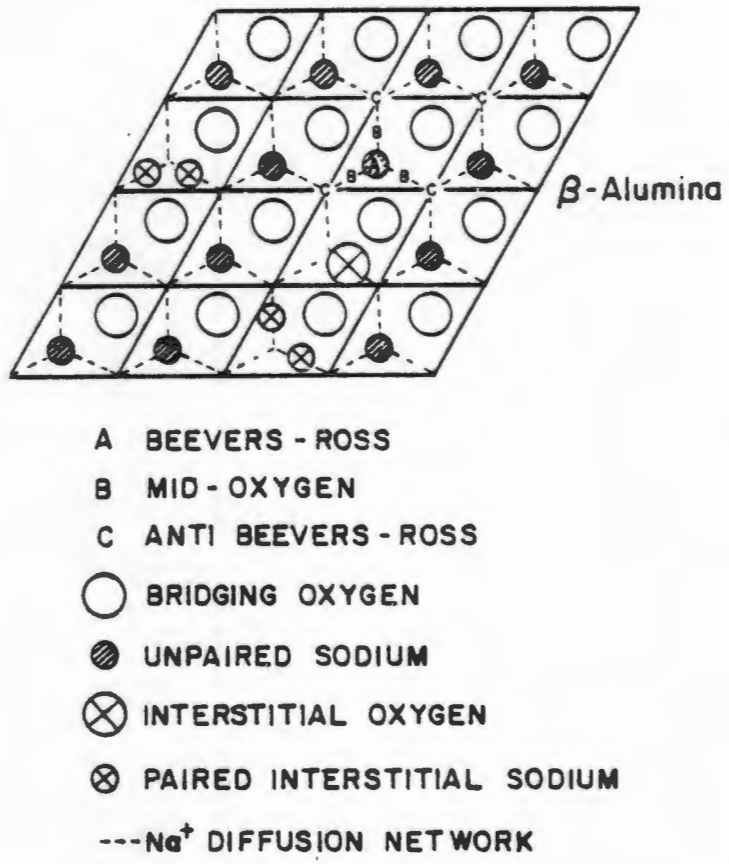

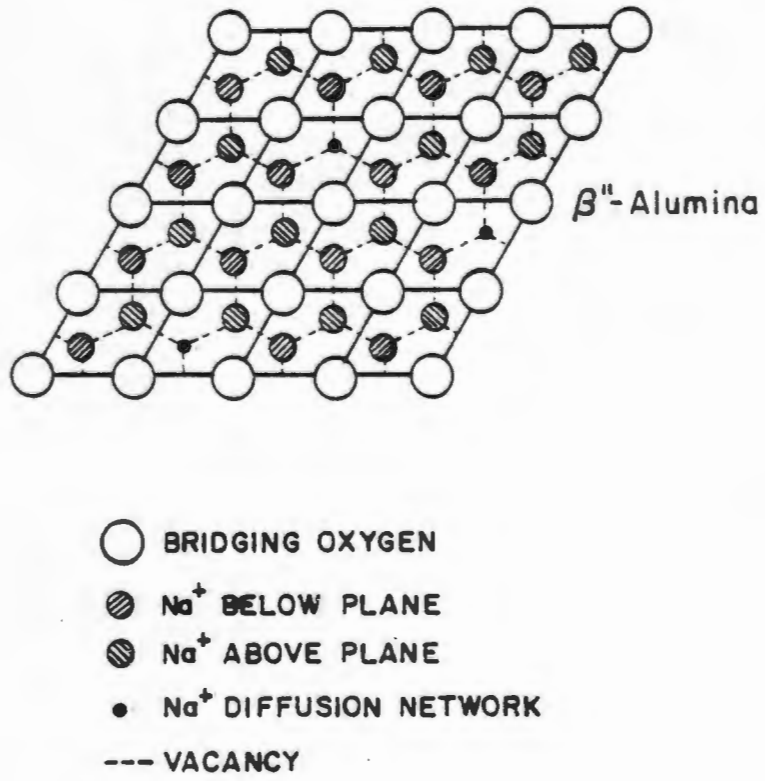

FIGURE 1.4: The Na ion sites in the conduction planes of β- and β"-Al_2O_3 (after Mosely 1985)

TABLE 1.1: Representative crystallographic information for the β-Al_2O_3 structure (Peters et al. 1971)

Hexagonal P $6_3/mmc$

Lattice parameters for a specimen with 6,6 wt% Na_2O, i.e. $(Na_2O)_{1.29}11Al_2O_3$: a = 5,594 Å, c = 22,53 Å

Calculated density = 3,25 g cm^{-3}

Atomic positional parameters

Atom	Number of equivalent positions Wyckoff notation	Type of site	x	y	z
O(1)	12(k)	tetrahedral	0,157	$\bar{x}$	0,050
O(2)	12(k)	tetrahedral	0,503	$\bar{x}$	0
O(3)	4(f)	tetrahedral	1/3	2/3	0,056
O(4)	4(e)	tetrahedral	0	0	0,143
O(5)	2(c)*	linear	1/3	2/3	1/4
Al(1)	12(k)+	octahedral	0,832	$\bar{x}$	0,106
Al(2)	4(f)	tetrahedral	1/3	2/3	0,025
Al(3)	4(f)	tetrahedral	1/3	2/3	0,176
Al(4)	2(a)	octahedral	0	0	0
Na(1)	2(c)*	BR++	2/3	1/3	1/4
Na(2)	6(h)	mO**	0,873	$\bar{x}$	1/4

* These sites refine best when split into 6h sites with 1/3 occupancy on each

\+ This site is only partly occupied. The balance of the Al atoms switch to a Frenkel defect site near 0,832 x 0,176 and stabilize an interstitial oxygen near to an mO site

++The Beevers-Ross (1937) site. Here occupied ~1,5 per unit cell

**The mid-oxygen site. Here occupied ~1,0 per unit cell.

Mean aluminium-oxygen distances

Atom	Co-ordination number	Mean Al-O (Å)
Al(1)	6	1,92
Al(2)	4	1,80
Al(3)*	4	1,75
Al(4)	6	1,90

* Constituting part of the Al-O-Al spacer column.

TABLE 1.2: Representative crystallographic information for the β''-Al_2O_3 structure (Jorgensen 1981)

Rhombohedral $R\bar{3}m$

Lattice parameters referred to hexagonal axes for a specimen with 8,85 wt% Na_2O, 0.75 wt% Li_2O, i.e. $Na_{1,72}Al_{10,66}Li_{0,30}O_{17}$
a = 5,610 Å, c = 33,463 Å

Calculated density = 3,28 g cm^{-3}

Atomic positional parameters

Atom	Number of equivalent positions Wyckoff notation	Type of site	x	y	z
O(1)	18(h)	tetrahedral	0,155	$\bar{x}$	0,034
O(2)	18(h)	tetrahedral	0,164	$\bar{x}$	0,235
O(3)	6(c)	tetrahedral	0	0	0,296
O(4)	6(c)	tetrahedral	0	0	0,098
O(5)	3(b)	linear	0	0	1/2
Al(1)	18(h)	octahedral	0,167	$\bar{x}$	0,929
Al(2)	6(c)*	tetrahedral	0	0	0,350
Li	6(c)*	tetrahedral	0	0	0,350
Al(3)	6(c)	tetrahedral	0	0	0,450
Al(4)	3(a)	octahedral	0	0	0
Na(1)	6(c)	BR/aBR+	0	0	0,828
Na(2)	18(h)	mO++	0,104	$\bar{x}$	0,834

* Site occupied by Al/Li in the ratio 1,71/0,29

\+ In the β''-Al_2O_3 structure the Beevers-Ross (BR) and anti-Beevers-Ross (aBR) sites are crysallographically equivalent. Here occupied ~1,32 per unit cell

++The second set of sodium positions occurs in pairs (only one of which can be occupied) centred on the mid-oxygen site. Here occupied ~3,69 per unit cell

Mean aluminium-oxygen distances

Atom	Co-ordination number	Mean Al-O (Å)
Al(1)	6	1,91
Al(2)	4	1,85
Al(3)*	4	1,74
Al(4)	6	1,89

* Constituting part of the Al-O-Al spacer column.

1.3 PHASE RELATIONSHIPS

A comprehensive phase diagram for the Na_2O-Al_2O_3 system based on previous literature was suggested by De Vries and Roth (1969). It is assumed that β''-Al_2O_3 is metastable in the binary system, forming at around 1100 °C and irreversibly decomposing to β-Al_2O_3 and δ-$NaAlO_2$ above 1550 °C. Subsequent phase diagrams for the binary system have been published by Weber and Venero (1970) and by Le Cars et al. (1973). Figure 1.5 represents the most recent phase diagram for the binary system suggested by Le Cars et al. (1973). The hatched region corresponds to the existence of both β-Al_2O_3 and β''-Al_2O_3 phases.

Dopant ions with an ionic radii between 0.6 and 0.9 Å such as lithium, cobalt, magnesium and zinc stabilize the β''-Al_2O_3 structure at high temperatures. These dopants substitute for the tetrahedrally co-ordinated aluminium on site Al(2) (see Table 1.2) and occupy this site with less strain than the smaller aluminium ion. An application of Pauling's rules, (Pauling, 1963), to the stoichiometric β''-Al_2O_3 structure indicates that there is an aggregation of positive charge at the centre of the spinel blocks and a negative charge at the walls of the conduction planes. West (1979) has suggested that the substitution of the tetrahedrally co-ordinated aluminium ion on Al(2) sites by a larger monovalent or divalent cation such as lithium or magnesium would equalize the charge distribution in the spinel block and thereby stabilize the β''-Al_2O_3 phase.

The ternary phase diagram for Na_2O-Li_2O-Al_2O_3 was published by Duncan and West (1983). Figure 1.6 is a revised diagram of the ternary system indicating the area of β''-Al_2O_3 stability at 1500 °C (Duncan 1985).

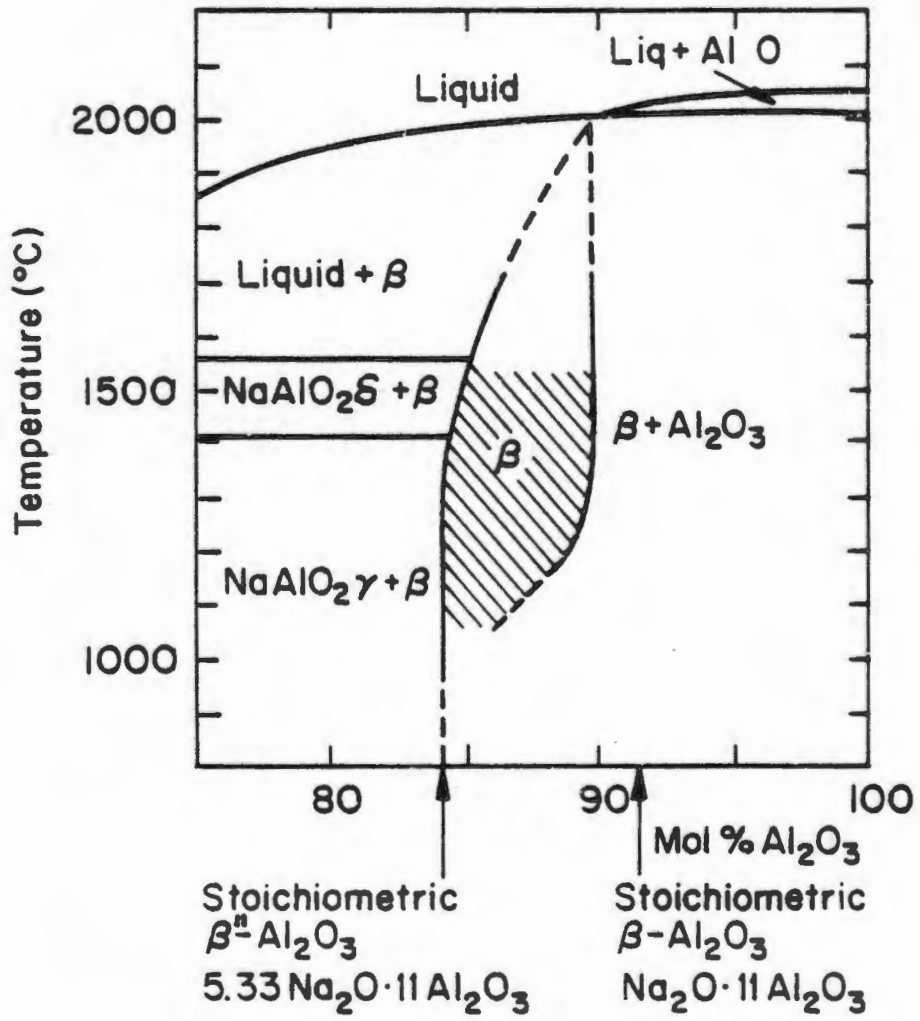

FIGURE 1.5: The phase diagram for the soda-alumina system Le Cars et al. (1973)

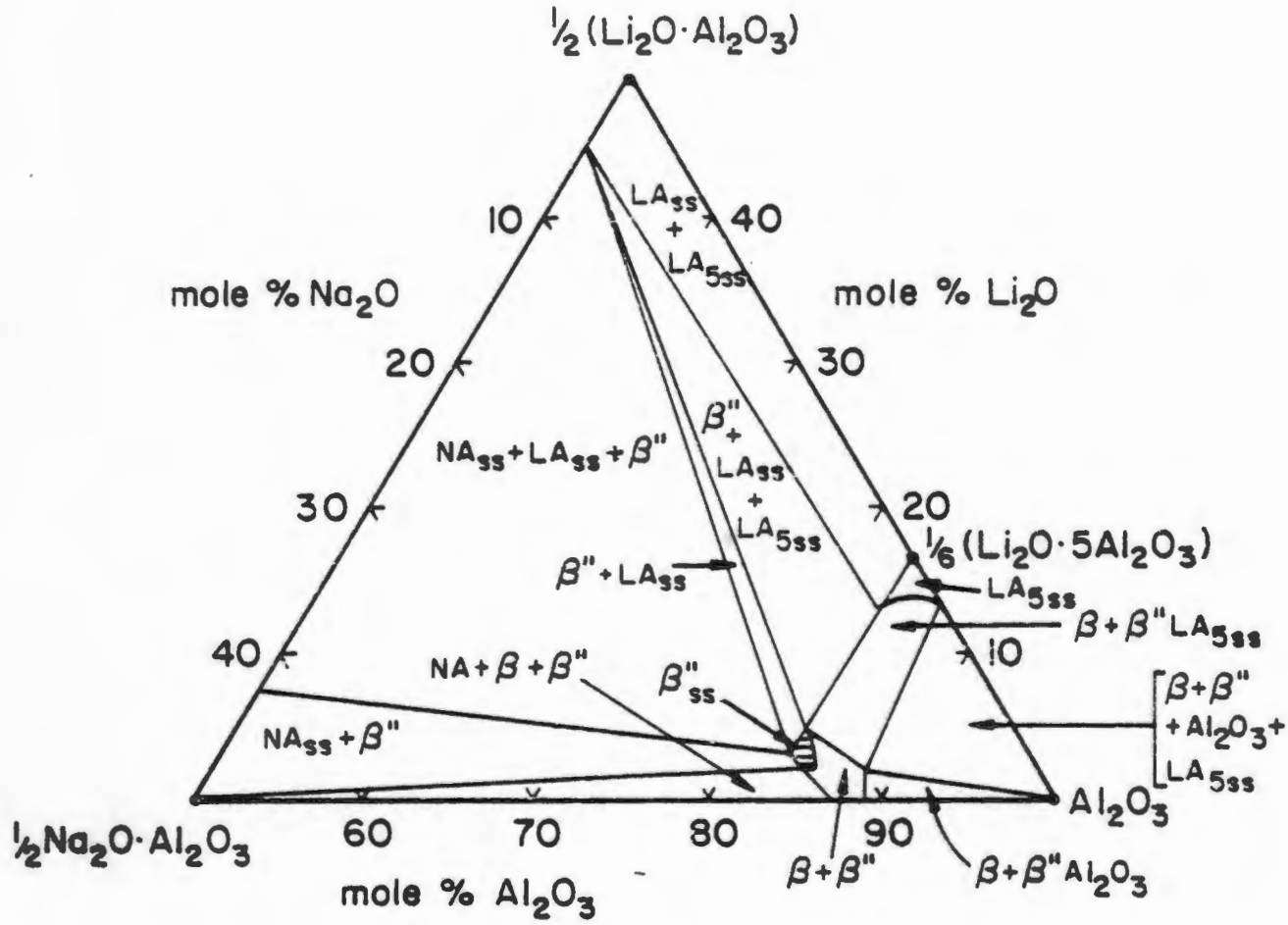

NA - $NaAlO_2$

LA - $LiAlO_2$

LA_5 - $LiAl_5O_8$

β - β-Al_2O_3

β" - β"-Al_2O_3

ss - Solid solution indicating non-stoichiometric compounds

FIGURE 1.6: The revised ternary phase diagrams for the soda lithia-alumina system (Duncan 1985)

1.4 THE FABRICATION OF BETA ALUMINA TUBES

The beta alumina tubes used in high energy density cells need to meet stringent requirements of structural integrity, dimentional control and ionic conduction properties. To obtain this combination of properties within closely defined cost goals, requires a sound understanding of the processing and property relationships of this material.

The fabrication of beta alumina consists of three principle stages. The first stage consists of powder preparation starting with an intimate mixture of precursor powders which are reacted at about 1200 °C to form beta alumina powder. The second step consists of powder consolidation into the required shape (green body). The last step of the process is high temperature sintering, which produces a dense polycrystalline material. The performance and properties of the artefact are strongly dependent on all the above processing steps. A review of each processing step follows.

Beta alumina powder has been prepared by the mechanical mixing of α-Al_2O_3 with salts of sodium and stabilizer dopants such as magnesium or lithium which were subsequently reacted to produce a powder of the desired composition. An example of this approach is the ball milling of α-Al_2O_3, Na_2CO_3 and $LiNO_3$ under acetone as described by Johnson et al. (1979). Reactant diffusion distances during reaction are limited by the mean particle size of the precursor mix. This method requires high reaction temperatures and subsequent milling of the reaction product. Furthermore material with poor dopant distribution is produced.

Increased dopant distribution is achieved by the use of the zeta process (Vikar et al., 1978). This process starts with the preparation of the zeta $LiAl_5O_8$ spinel by the solid state reaction of α-Al_2O_3 and an appropriate Li salt. The zeta

spinel is then ball-milled with a sodium salt and α-Al_2O to form beta alumina powder of desired composition.

Large quantities of beta alumina powder can be prepared conveniently by the spray drying of a milled, 50% solids content, aqueous slurry containing α-Al_2O_3, soluble sodium and stabilizer salts. Vogel et al. (1981) demonstrated that this method produces a powder which is suitable for reaction sintering.

A number of chemical synthesis techniques for beta alumina production have been reported. These techniques are aimed at attaining a more homogeneous mix of reactants and include the use of metal alkoxide precursors [Morgan (1976), Yoldas and Pantlow (1980)], sol-gel processing [Gordon (1976), Chandry and Cannon (1978)] and solution spray freezing [Green and Hutchinson (1980), Pekarsky and Nicholson (1980)].

Beta alumina tubes have been formed by dry bag isostatic pressing [Deplanches (1980)], extrusion [Pett et al. (1982)], slip casting [Byckalo et al. (1976)] or electrophoretic deposition [Powers (1975)]. In a recent review [Duncan (1985)] it was reported that at present the only feasible forming techniques are electrophoretic deposition and dry bag isostatic pressing. The other techniques do not produce tubes with sufficiently high sintered densities.

Beta alumina is usually sintered above 1 585 ^{o}C, the binary eutectic, to achieve acceptable densities (above 3,16 g/cm^3). Sintering techniques need to overcome three problems:

i) soda evaporation
ii) development of duplex microstructures, and
iii) maintenance of high proportions of β''-Al_2O_3 phase.

Soda loss can be minimized by encapsulation in magnesia tubes [Sudworth (1975)], platinum [Youngblood et al. (1977)] or by the use of beta alumina setter powders [Fally et al. (1973)].

Exaggerated grain growth, resulting in a duplex microstructure can be repressed by rapid sintering in a zone furnace [Tan and May (1977)]. In this process grain growth is repressed but conversion to β''-Al_2O_3 must be allowed for in a post-sintering annealing stage [May (1978)].

In conventional batch sintering the duplex microstructure is avoided by the use of the double peak sintering schedule suggested by Duncan and Bugden (1981).

CHAPTER 2:

2.1 INTRODUCTION

Conventionally, beta alumina powders are synthesized by the solid state reaction of a high purity α-Al_2O_3 with suitable soda and lithia precursors. This synthesis technique has two principle disadvantages: The reaction product contains a mixture of β-Al_2O_3 and β''-Al_2O_3 and requires a double peak firing schedule to maximize the β''-Al_2O_3 content [Duncan and Bugden (1981)]. High purity α-Al_2O_3 is relatively expensive and recent cost models have shown that approximately a third of the total electrolyte cost can be ascribed to the α-Al_2O_3 raw material cost [Conradi (1986)]. The high cost derives from purification (soda removal) and the calcination of the aluminium hydroxides above 1200 °C to produce high purity α-Al_2O_3.

Barrow (1986) and Van Zyl et al. (1985a) reported that certain aluminium hydroxides can be used to synthesize β''-Al_2O_3 powders without intermediates at 1200 °C when reacted with sodium and lithium salts. No systematic study of the use of aluminium hydroxides for the preparation of beta alumina powders has been reported. This thesis deals with the synthesis and characterization of beta alumina powders derived from a range of synthetic aluminium hydroxide materials. As an introduction to the study, Chapter 2 contains a review of the classification, structure, phase relationships, dehydroxylation and reordering sequences of the aluminium hydroxide materials. Finally a review of the reported crystallization mechanisms of beta-alumina is presented.

2.2 CLASSIFICATION OF ALUMINIUM HYDROXIDES

The aluminium hydroxides can be divided into three catagories which are further subdivided as shown in Table 2.1. At present two sets of accepted nomenclature are applied to the aluminium hydroxides. Because of its familiarity the nomenclature suggested by Ginsberg et al. (1957) will be used. In the internationally accepted crystallographic nomenclature, the prefix α is applied to hexagonally close-packed and related structures, while the phases prefixed by γ, denote cubic close-packed lattices or structural elements of this symmetry. An alternative nomenclature suggested by Weiser and Milligan (1934) extends this convention to aluminium hydroxides.

TABLE 2.1: The catagorization of aluminium hydroxides

	Ginsberg et al. (1957)	Weiser & Milligan (1934)
Amorphous-alumina hydrates	"X-ray indifferent"	Amorphous
Aluminium Oxide Hydroxides (AlOOH)	boehmite	γ-aluminium monohydrate
	diaspore	α-aluminium monohydrate
Aluminium Trihydroxides ($Al(OH)_3$	gibbsite or hydragllite	γ-aluminium trihydrate
	bayerite	α-aluminium trihydrate
	nordstrandite	-

The aluminium hydroxides are important commercial products and are obtained by the chemical treatment of bauxite ores in the Bayer process. Each aluminium hydroxide will be discussed with reference to its preparation, occurrence and structure.

2.2.1 Amorphous alumina hydrates

The first attempt to classify aluminium hydroxides derived from gels was made by Willstütter et al. (1925) who distinguished between three forms C_α, C_β and C_γ. According to Kraut et al. (1942), Fricke and Schmäh (1948), Souza Santos et al. (1953) and Watson et al. (1957), C_α is amorphous and the water content corresponds to a trihydroxide. Upon aging this material transforms to C_β which has structural elements similar to boehmite. After several weeks C_β can be converted to C_γ by aging in an alkaline solution. C_γ corresponds to a mixture of bayerite and boehmite.

The gels can be prepared in different ways:

According to Torkar and Egghart (1961), the hydrolysis of $Al(OC_2H_5)_3$ at 0 °C yields an "X-ray indifferent" product. The gel can be made to transform to bayerite or boehmite by hydrothermal treatment. Teichner (1953) prepared pure amorphous aluminas by the action of water vapour or heat on aluminium methylate. The water content of the amorphous materials varies with the temperature of treatment. Precipitates from aluminium methylate decomposed at low temperature, had a surface area of 300 m^2g^{-1}, and an X-ray pattern with weak halos at 4, 5, 2, and 1,4 Å. Papée et al. (1958) described an amorphous alumina gel prepared by precipitation of aluminium nitrate at pH 8 with ammonia, followed by rapid washing and drying under vacuum at 25 °C to constant weight. The composition of the product was $Al_2O_3 \cdot 3{,}45H_2O$. Its surface area was 170 m^2g^{-1}. It showed a broad X-ray band at ~1,4 Å.

Except for material prepared at a pH above 7, or at elevated temperatures, the initial product is always "X-ray indifferent". Petz (1968) investigated the structure of the amorphous precipitates by X-ray scattering techniques. According to this author, aluminium ions are surrounded by six oxygen

atoms in octahedral configuration. This is the same coordination as in crystalline oxides or hydroxides. Since hydrogen has a low X-ray scatter cross-section, the data does not differentiate between O, (OH), and H_2O. The second nearest neighbours of the aluminium ion are arranged in tetrahedral configuration, similar to that in liquid water. Marboe and Bentur (1961) postulated that in aqueous solutions of Al ions the nearest and second nearest neighbours are H_2O molecules. Adding a base to the solution will extract protons from the hydration shells. As a result, dipolar ions form which cluster together. The authors considered the initially-formed gel not to be a hydroxide, but rather a distorted water matrix immobilized by Al and (OH) ions. For each (OH)-site occupied by an H_2O molecule the clusters (micelles) retain a positive charge. This explains the strong adsorption of anions by freshly-precipitated gels.

Transformation to crystalline hydroxide (aging) is controlled by the rate of replacement of H_2O by (OH) ions. The final product of the aging process is crystalline $Al(OH)_3$, if the (OH) concentration is sufficiently high.

According to Ginsberg et al. (1961), Lippens (1961) and Bye and Robinson (1964), boehmite occurs as the first X-ray crystalline form in the aging sequence. It is assumed by Feinknecht et al. (1961) that boehmite is formed by a topochemical reaction. This can be explained by the mechanism proposed by Marboe and Bentur (1961): The micelles, i.e. the initially-formed solid, contain (OH) and H_2O in varying proportions. If an (OH) ion reacts topochemically with another (OH), rather than replacing an H_2O, a new water molecule is formed, leaving an oxygen ion in the solid:

$$Al\text{-}(OH) + (OH) \rightarrow Al\text{-}O + H_2O$$

Consequently, the micelles are transformed to Al $[(O)\text{-}(OH)\text{-}(H_2O)]$ complexes, a composition which corresponds with the idealized formula for pseudoboehmite.

2.2.2. Aluminium Oxide Hydroxides

2.2.2.1 Boehmite and Pseudoboehmite

Aluminium oxide hydroxides can be precipitated by neutralizing aluminium salt or aluminate solutions at temperatures near and above the boiling point of water. Treating amalgamated (activated) aluminium with boiling water is another method of preparation. The reaction product formed on the surface of the aluminium metal consists of "X-ray indifferent" material and pseudoboehmite i.e., the poorly crystallized hydrated form.

Pseudoboehmite is often confused with the chemically and structurally different well-crystallized boehmite and there is some disagreement in literature on the occurrence of boehmite at low and moderate temperatures. The diffraction pattern of pseudoboehmite shows broad bands which coincide with the strong reflections of the well-crystallized material. Papée, Tertian and Biais (1958) studied the differences between well-crystallized hydrothermally prepared boehmite, and pseudoboehmite. They pointed out that pseudoboehmite cannot be considered simply a finely divided or poorly crystallized aluminium oxide hydroxide. The difference in structure was indicated by the strong variation in the 020 X-ray reflection, which increased from 6,11 A for crystalline boehmite to between 6,6 and 6,7 A for the pseudoboehmite forms. Furthermore, the X-ray pattern did not show the usual modifications observed for distorted crystals. In hydrothermal evolution experiments, pseudoboehmite was progressively converted to crystalline boehmite. Even under mild conditions (18 hours at 200 °C), there was a significant shift of the 020 X-ray reflection from 6,6 to 6,19 A and a substantial decrease of the excess water from 60 to 12%. Under more severe conditions (18 hours at 285 °C), the excess water fell to 1%, while the X-ray pattern showed only slight differences from

that of the crystalline boehmite. After a treatment of 48 hours at 300 °C, pseudoboehmite reached the theoretical composition of AlOOH and showed an X-ray pattern similar to crystalline boehmite. The excess water is thus not to be considered as merely adsorbed at the surface of a finely divided solid; it is rather situated between the elemental structure layers, thus leading to an enlargement of the basal spacings.

Samples of pseudoboehmite usually contain water in excess of the theoretical 15%. Goton (1955) proposed that this water is probably bound as $Al(OH)_3$. But Tertian and Papée (1958) do not accept this hypothesis. They considered the excess water as intercrystalline, thus suggesting a fundamental difference in structure between boehmite and pseudoboehmite.

Formation of boehmite by a solid state reaction has been observed when gibbsite is heated in air to temperatures between 110 and 300 °C. Conversion of the trihydroxide to measurable amounts of boehmite requires the rapid heating of coarse particles. It is therefore assumed that high water vapour pressures generated within large gibbsite grains during rapid dehydroxylation lead to the formation of the aluminium oxide hydroxide. Gibbsite heated above 100 °C under water or dilute alkaline solutions is quantitatively converted to boehmite.

The structure of boehmite as described by Ewing (1935), Reichartz and Fost (1946), and Milligan and McAtee (1956) consists of layers which are composed of chains formed by double molecules of AlOOH which extend in the direction of the a-axis. Hydroxyl ions of one double layer are located over the depression between hydroxyl ions in the adjacent layers. The double layers are linked by hydrogen bonds between hydroxyl ions in neighbouring planes. Average O-O distance of the hydrogen bridges is 2,70 Å. Boehmite crystals

exhibit perfect cleavage perpendicular to the general direction of the hydrogen bonding.

2.2.2.2 Diaspore

Since diaspore is usually associated with older bauxites and metamorphic rocks, high pressure and elevated temperature are considered necessary for the formation of this mineral. The hydrothermal synthesis of diaspore by Laubengayer and Weiss (1943) at temperatures above 400 °C seemed to confirm this theory.

In diaspore the oxygen ions are nearly equivalent, each being joined to one other oxygen by way of a hydrogen ion and being arranged in hexagonal close packing. In the hydrogen bridges the O-O distance is 2,65 Å. The compact arrangement explains the greater density of this oxide hydroxide and the low frequency of the OH-stretching vibration shown by infrared absorption.

Diaspore is the only aluminium hydroxide which converts directly to α-alumina upon heating. This phenomena is related to the hexagonal packing arrangement of the oxygen atoms.

2.2.3 Aluminium Trihydroxides

2.2.3.1 Gibbsite

Gibbsite usually contains a few hundredths to several tenths of a percent of alkali metal ions. The highest alkali concentrations are found in technical trihydroxides produced in the Bayer process. Ginsberg and Köster (1952) and Wefers (1965) showed that sodium is atomically dispersed in the crystal lattice of gibbsite. Occlusions of solid NaOH in the grains were not detected.

There is strong evidence in the literature, [Ginsberg et al. (1962), Torkar et al. (1960), Saalfeld et al. (1968)], that alkali metal ions are necessary to stabilize the gibbsite structure. This mineral should therefore not be considered a pure aluminium trihydroxide, but rather a ternary compound.

The structure was determined by Megaw (1934) and was later refined by Saalfeld (1960). Gibbsite is usually monoclinic with a space group $P2_1/n$, or C^5_{2h}. Double layers of OH ions, with Al ions occupying two thirds of the octahedral interstices within the layers, form the basic element of this lattice. Each double layer is positioned with respect to its upper and lower neighbours in such a way that hydroxyl ions of adjacent planes are directly opposite each other. Thus, the sequence of OH ions in the direction perpendicular to the planes is [..AB BA AB BA..]. This superposition of layers and the hexagonal arrangement of the Al ions leads to channels through the lattice parallel to the c-axis. Hydrogen bridges, originating from the dipoles, operate between OH groups of adjacent double layers.

2.2.3.2 Bayerite

Fricke and Wullhorst (1932) prepared bayerite by neutralization of a sodium aluminate solution with carbon dioxide at 20 °C. According to Fricke and Jockers (1947) bayerite is also obtained by hydrolysing aluminium alcoholates at temperatures below 40 °C. Torkar and Bergmann (1960) produced extremely pure bayerite electrolytically, using platinum cathodes, aluminium anodes and H_2O_2 as an electrolyte.

A method of preparing well-crystallized bayerite was described by Schmäh (1946). This author immersed slightly amalgamated aluminium in water for several days. According to Lippens (1961), this method gives the best results when the water is free of electrolytes and has a pH of 7.

The crystal lattice of bayerite is composed of layers of hydroxyl ions similar to those in gibbsite. These layers are, however, arranged in an [...AB AB AB...] sequence; hydroxyl ions of the third layer lie in the depressions between OH positions of the second one. Although the arrangement corresponds to a hexagonal close packing of spheres, the symmetry of bayerite is monoclinic, space group $P2_{1/n}$ or C^5_{2h} [Unmack (1951)].

Rothbauer, Zigan and O'Daniel (1967) refined the bayerite structure by X-ray powder and neutron diffraction measurements. The authors confirmed the space group determined by Unmack (1951). They proposed a distribution of hydrogen according to which approximately one third of the hydrogen atoms occupy octahedral interstices within the double layers. Two thirds of the existing octahedral voids are filled by aluminium. The remaining hydrogen atoms are located in tetrahedral interstices between two double layers, acting as hydrogen bridges.

2.2.3.3 **Nordstrandite**

Van Nordstrand, Hettinger and Keith (1956) published an X-ray diagram of an aluminium trihydroxide which differed from the diffraction patterns of gibbsite and bayerite. They obtained this trihydroxide by precipitating a gel from aluminium chloride or nitrate solutions with ammonium hydroxide.

Upon aging under the mother liquor at a pH of 7,5 to 9 the gel converted to the crystalline phase. Van Nordstrand proposed the name bayerite II, since structure and growth features were closely related to those of bayerite. In honour of the author, this trihydroxide was later called nordstrandite.

Saalfeld and Jarchow (1968) refined the structure, pointing out that the sequence of layers is [...AB AB AB...] as in

bayerite; on the other hand, OH ions of adjacent double layers are located opposite each other. This places the lattice of nordstrandite between those of bayerite and gibbsite.

Although the technical production of nordstrandite is covered by patents [Hauschild 1964 (a) (b)], the material has not been used commercially to date.

2.3 PHASE RELATIONSHIPS IN THE ALUMINA - WATER SYSTEM

The aluminium hydroxides, $Al(OH)_3$, and AlOOH and Al_2O_3 are the compositions of the three groups of aluminium compounds which exist in the alumina - water binary system.

The stability relationships of bayerite, gibbsite and nordstrandite have been investigated by Ginsberg et al. (1961) and it has been shown that bayerite is the most stable trihydroxide. Wefers (1967) has also pointed out that gibbsite does not have a field of stability in the Al_2O_3-H_2O binary system since all the samples investigated contained sodium ions in the lattice.

The mutual stability relationships of the aluminium trihydroxides can be explained from a structural point of view. As demonstrated, the structures of gibbsite, bayerite and nordstrandite differ only in the stacking sequence of a common structural element, the $Al_2(OH)_6$ layer. All main valencies of the $Al_2(OH)_6$ are satisfied within the layer. Only relatively weak forces operate between the layers. It has been shown in the preceding sections that the method of preparation determines the structure and the degree of crystallinity of the final product. Neither gibbsite nor nordstrandite can be prepared free of impurities [Hauschild (1963)], suggesting that foreign ions or molecules included in the lattice affect the stacking sequence of the $Al_2(OH)_6$ layers.

The phase diagram for the Al_2O_3-H_2O system was first published by Ervin and Osborn (1951) and was later modified by Kennedy (1959). Neuhaus and Heide (1975) confirmed Kennedy's phase diagram.

Under hydrothermal conditions $Al(OH)_3$ transforms to AlOOH at approximately 100 °C. No differences in the temperature of conversion have so far been reported for bayerite, gibbsite or nordstrandite. Below 300 to 320 °C the spontaneously crystallizing phase is boehmite. Ginsberg and Köster (1952) found that sodium ions, i.e. a slight alkalinity of the solution, considerably increased the rate of transformation to boehmite.

Spontaneous growth of diaspore occurs above 300 °C and 200 bar pressure. Using natural diaspore as a seed, Laubengayer and Weiss (1943) transformed boehmite to diaspore at 280 °C under the pressure of saturated water vapour. In hydrothermal experiments, Neuhaus and Heide (1975), grew diaspore from mixtures of boehmite and diaspore above 180 °C. The reverse reaction was never observed. They concluded that boehmite is metastable but kinetically favoured at low temperatures and pressures.

From the phase information it is clear that all the trihydroxides can be converted to the boehmite by hydrothermal treatment. Large crystals of the trihydroxides also transform to boehmite because of the micro-autoclaving conditions created by the accumulation of steam within the crystallites during the early stages of dehydroxylation.

Thermal analysis combined with X-ray diffraction studies have confirmed this hypothesis.

2.4 THERMAL DEHYDROXYLATION AND SUBSEQUENT REORDERING OF ALUMINIUM HYDROXIDES

When the aluminium hydroxides are heated, more than 98 per cent of the lattice water is removed below 600 °C. Before transformation to α-alumina occurs at 1200 °C, the aluminium hydroxides proceed via a series of irreversible transition aluminas. The interrelationship between the aluminium hydroxides and the transition alumina forms is presented in Table 2.1.

A general mechanism for the thermal decomposition of aluminium hydroxides has been proposed. The first step involves the diffusion of protons between the layers [Feinknecht et al. (1961)] which then react with the bridging OH groups to form water [Freund 1967)]. This process removes the binding forces between the strata causing chemical, physical and structural changes within the layers. Separation of the layers, distortion of the octahedra as well as the formation of areas of short range order are the result. The proton mobility is determined by the nature of the hydroxides, the presence of foreign ions, the distance between the layers (basal spacing) and the registry between the adjacent layers.

It has been reported that several variables influence the nature of the structural transformations of the aluminium hydroxides when heated. The transformations are influenced by the pressure, atmosphere, heating rate and particle size of the starting material. The influence of these variables on the transformations is depicted in Table 2.1.

The dehydroxylation and structural transformations of the aluminium hydroxides have been extensivly reported by Goton (1955) and Lippins (1961) (well-crystallized boehmite), Abrams and Louw (1969) (pseudoboehmite), Torkar and Egghardt (1961) (bayerite) and Eyrand (1965) (gibsite). The detailed transformations are shown in Table 2.1.

The transition aluminas cannot be considered to be polymorphs of Al_2O_3 as the materials contain small amounts of hydrogen ions which impart their unique structures. The transformation sequences are not reversible as none of the high temperature forms can be converted to lower temperature forms. Transition aluminas can be regarded as thermodynamically unstable, reasonably reproducible, states of structural reordering existing between the aluminium hydroxides and α-alumina. This view is supported by the fact that the nature of the aluminium hydroxide starting material determines thermal decomposition behaviour and the type and sequence of intermediate aluminas formed.

The first systematic structural classification of the transition aluminas was published by Stumpf (1950). The transformation sequences are influenced by many variables and considerable difficulty in the interpretation of X-ray patterns arises because of the similarity and broadness of the reflections. Electron and neutron diffraction techniques are more suitable for the study of the intermediate structures but it has been reported by Ginsberg et al. (1961) that electron bombardment under high vacuum causes a change in the outer layer of the sample under investigation, thereby influencing the results. A summary of the structural properties of the transition aluminas is presented in Table 2.2.

Krischner (1971) categorized the dehydroxylation products (transition aluminas) of the aluminium hydroxydes according to the oxygen stacking order of the materials. An α-, β- and γ-series was identified. Diaspore belongs to the α series with an [..AB AB..] stacking of the oxygen sublattice. Gibbsite, when dehydroxylated produces material with a [..ABAC ABAC..] sublattice and is classified as a β-series material. When dehydroxylated, hydrothermal boehmite, bayerite and nordstrandite produce materials belonging to the γ-series with an [..ABC ABC..] oxygen sublattice stacking.

TABLE 2.1: Composition sequence of aluminium hydroxides

Conditions	Conditions favouring transformations Path a	Path b
Pressure	>1 atm.	1 atm.
Atmosphere	Moist air	dry air
Heating rate	>1 °C/min	<1 °C/min
Particle size	>100 microns	<10 microns

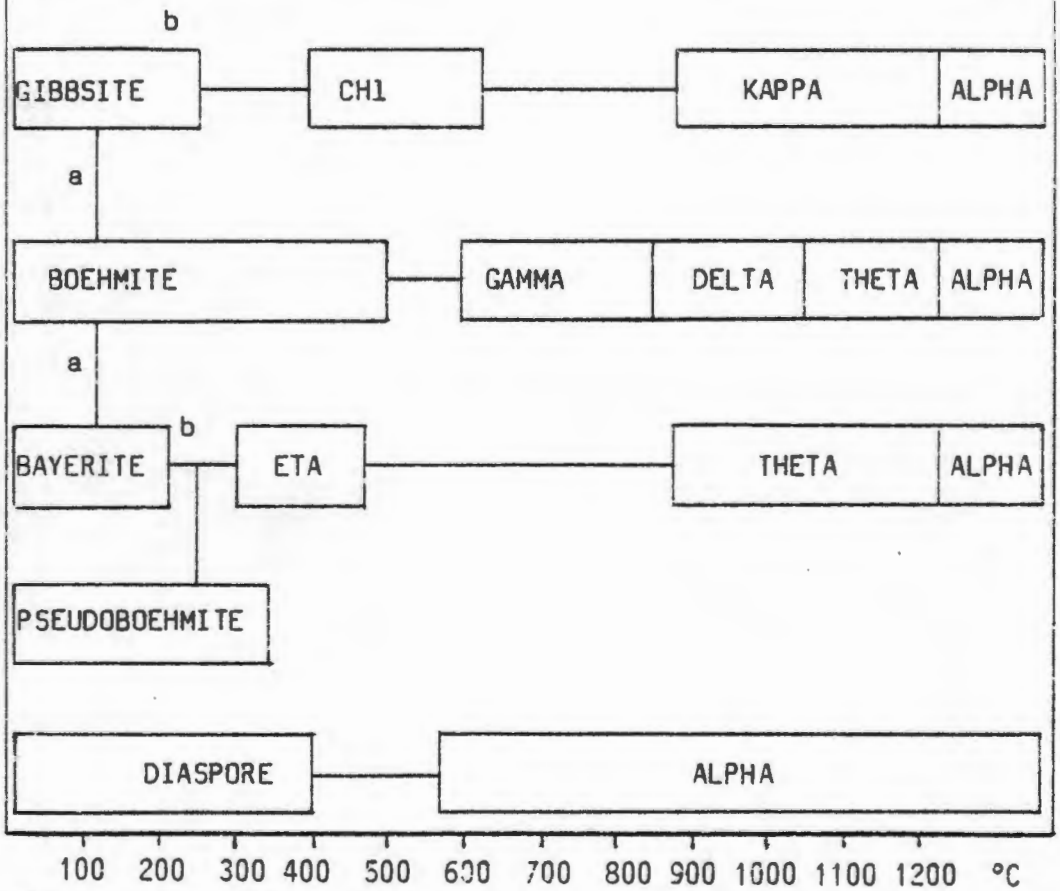

Note: Enclosed area indicates range of occurrence. Open area indicates range of transition.

TABLE 2.2: Structural properties of transition aluminas

FORM	CRYSTAL SYSTEM	SPACE GROUP	MOLECULES PER UNIT CELL	UNIT AXIS LENGTH, A			ANGLE	DENSITY g cm
				a	b	c		
Gamma	Tetragonal	-	-	5,62	7,80	-	-	3,2
Delta	Orthorhombic	-	12	4,25	12,75	10,21	-	3,2
	Tetragonal	-	-	7,96	-	23,4	-	-
Eta	Cubic (Spinel)	O	10	7,90	-	-	-	2,5-3,6
Theta	Monoclinic	C	4	11,24	5,72	11,74	103°20	3,56
Chi	Cubic	-	10	7,95	-	-	-	2,0
	Hexagonal	-	-	5,56	-	13,44	-	-
	Hexagonal	-	-	5,57	-	8,64	-	-
Kappa	Hexagonal	-	28	9,71	-	17,86	-	3,1-3,3
	Hexagonal	-	-	9,70	-	17,86	-	-
	Hexagonal	-	-	16,78	-	17,86	-	-
Iota	Orthorhombic	-	4	7,73	7,78	2,92	-	3,71
	Orthorhombic	D or C	3	7,59	7,67	2,87	-	3,0

2.5 BETA ALUMINA CRYSTALLIZATION PATHWAYS

Some suggested mechanisms by which beta alumina is formed when alumina or certain of its precursors are reacted with soda and stabilizer ions have been reported.

A crystallization pathway often observed by workers preparing β-Al_2O_3 by chemical synthesis [Takahashi and Kuwabara (1980)] involved the formation of a m-Al_2O_3 phase. Intermediate m-Al_2O_3 has a structure in which the sodium ions occupy interstitial positions in alternate oxygen close-packed layers in a mullite-like lattice. A prerequisite for the formation of m-Al_2O_3 phase is atomic mixing of the reactants. The existance of m-Al_2O_3 is often used as a criteria for determining how well the reactants are mixed prior to reaction. Hodge (1983) observed that the hydrolysis of a mixed (Al Mg) alkoxide in the presence of a sodium alkoxide produced m-Al_2O_3 at about 600 °C. At 700 °C most of the m-Al_2O_3 had transformed to β-Al_2O_3. At 1200 °C the powder contained pure β-Al_2O_3.

The preferred β"-Al_2O_3 phase is stabilized by the addition of small amounts of Li_2O or MgO to the Al_2O_3 and Na_2O reaction mixture. On the basis of a dilatometric and X-ray diffraction study, Bugden and Duncan (1979) suggested that the solid state reaction of 84 mole per cent α-Al_2O_3 with 13 mole per cent Na_2O and 3 mole per cent Li_2O produced a sodium aluminium intermediate at 800 °C. At a temperature of about 1150 °C the sodium aluminate reacted with some of the residual α-Al_2O_3 to form β-Al_2O_3 with a nominal composition of $Na_2O.11Al_2O_3$. Since the overall composition was $Na_2O.6Al_2O_3$ residual sodium aluminate was available. Above 1200 °C some β-Al_2O_3 was converted to β"-Al_2O_3 with the residual sodium aluminate disappearing. After heating at 1200 °C to equilibrium, the solid state reaction produces approximately 60 per cent β-Al_2O_3 and 40 percent β"-Al_2O_3. These results were

confirmed by Vogel et al. (1981) and subsequently by Hodge (1983) for powders containing α-Al_2O_3 and Na and Li salts. In none of the above cases XRD peaks corresponding to the lithium-rich phase were observed.

Another crystallization pathway produces the so-called intergrown β/β''-Al_2O_3 structure. The intergrown β/β''-Al_2O_3 structure is characterized by the fact that a powder XRD pattern of the material shows distinct peaks for the reflections which are common to β and β''-Al_2O_3 while the peaks which are unique to β''-Al_2O_3 and β-Al_2O_3 are poorly resolved and give rise to a diffuse reflection. The intergrown structure has been reported for materials that were synthesized from disordered transition aluminas (γ-Al_2O_3) [Poulieff et al. (1978)]. The disordered transition aluminas generally result from the low temperature calcination of chemically prepared alumina precursors. Poulieff et al. (1978) suggests that the α-$Al_2O_3 \rightarrow \beta$-$Al_2O_3$ transformation is topotactic. Such a mechanism requires the diffusion of sodium ions into the structure. The highly disordered γ-Al_2O_3 structure is retained and the stacking faults are inherited by the intergrown β-Al_2O_3.

This mechanism makes no reference to the form, if any, of a sodium aluminate intermediate and does not specify the diffusion mechanism (pore or solid state) of the sodium ions or the role of the lithium ions. Hodge (1983) postulated that the disordered γ-Al_2O_3 acts as a substrate for the epitaxial nucleation of β- and β''-Al_2O_3 followed by the growth of these phases. Sodium ions are transported by the β or β''-Al_2O_3 to the reaction interface. The model does not address the possibility of the formation of a sodium aluminate intermediate and does not adequately explain the reason for both β and β''-Al_2O_3 nucleation on the disordered γ-Al_2O_3 substrate. The role of the stabilizer ion is not referred to.

It is clear that no consensus exists on the nature of the reaction mechanisms by which β/β''-Al_2O_3 is formed from a disordered transition alumina. Furthermore, no systematic study of the synthesis of beta-alumina from a wide range of aluminium hydroxides has been reported. This thesis will attempt to relate the nature of the aluminium hydroxide precursor to the transition alumina formed upon dehydroxylation and ultimately to the nature of the resulting beta alumina powder formed upon reaction with soda and lithia.

CHAPTER 3

This chapter deals with the synthesis and characterization of a range of high purity aluminium hydroxides precursors from a common parent material. The physical and chemical properties as well as the dehydroxylation behaviour and crystallization pathways of the materials will be reported.

3.1 SYNTHESIS OF HIGH PURITY ALUMINIUM HYDROXIDE MATERIALS

Van Zyl et al. (1985b) indicated that commercial aluminium hydroxides show substantial variability with respect to impurity levels, preparation methods, dehydroxylation behaviour and particle size. In order to make a comparative study of the synthesis of beta alumina from aluminium hydroxide precursors, it was necessary to synthesize high purity, well-characterized aluminium hydroxide materials to eliminate the effects of the variations mentioned in the above.

Yoldas (1973) showed that the hydrolysis of aluminium alkoxides is a convenient method for the synthesis of high purity aluminium hydroxides. Aluminium alkoxides of high high purity with a general formula $Al(OR)_3$ can be synthesized by the technique reported by Bradley (1978): High purity (99.999%) Al metal is refluxed with excess isopropanol (doubly distilled spectrapure material) in the presence of trace amounts of $HgCl_2$ catalyst. The aluminium metal converts to aluminium isopropoxide after refluxing in teflon-lined containers for 24 hours. The reaction product is vacuum-distilled and recrystallized from high purity toluene to produce aluminium tri-isopropoxide. This material is subsequently hydrolysed with high purity water under different temperature and pressure conditions to produce a range of aluminium hydroxides.

The hydrolysis of aluminium isopropoxide was carried out in a reactor system described by Van Zyl et al. (1986a). In the initial experiments aluminium tripropoxide synthesized by the method of Bradley (1978) was used. An equivalent, commercial, high purity aluminium isopropoxide (99.999% purity Al metal base) was used in subsequent experiments.

The reaction system was used to produce pseudoboehmite and bayerite as reported by Yoldas (1973). Hydrothermal boehmite was produced by autoclaving the synthetic pseudoboehmite. α-Al_2O_3 was produced by calcining the pseudoboehmite at 1400 °C for 2 hours. As reported earlier, gibbsite always contains small amounts of sodium ions. Gibbsite was synthesized by a modified alkoxide hydrolysis technique. The synthesis and characterization of the materials are now discussed in detail.

A 0.5 molar stock solution of aluminium isopropoxide in doubly distilled iso-propanol was prepared and stored in a teflon-lined container under argon. A solution of 18 MΩ cm purity water was stored under argon in a teflon-lined vessel. Teflon-lined vessels were used to prevent silica contamination from glassware during storage.

Pseudoboehmite was synthesized by contacting 200 ml (0.1 moles) of preheated (80 °C) alkoxide stock solution with 300 ml (~16.6 moles) of preheated water in a static mixer, followed by stirring the resulting suspension in a jacketed vessel at 80 °C for 2 hours. The resulting suspension was aged for 24 hours at 20 °C and then centrifuged. After centrifuging the resulting gel was resuspended in distilled, deionized water. This procedure was repeated three times before drying in a laminar air flow hood at 120 °C.

High purity α-Al_2O_3 was made by heating a portion of the pseudoboehmite in a covered platinum crucible at 1400 °C for 2 hours.

Well-crystallized hydrothermal boehmite was synthesized by autoclaving a suspension of an equal mass of synthetic pseudoboehmite and 18 MΩ cm purity water in a teflon-lined autoclave for 24 hours at 200 °C and saturated steam pressure. The product was dried in a laminar air flow hood at 120 °C.

Bayerite was prepared by contacting 200 ml (0.1 moles) of pre-cooled (approximately 5 °C) alkoxide stock solution with 300 ml (16.6 moles) of pre-cooled water in a static mixer, followed by stirring the resulting suspension in a jacketed vessel at 5 °C for 2 hours. The vessel was cooled to prevent the exothermic hydrolysis reaction from heating the suspension above 80 °C, the temperature at which pseudoboehmite forms. After 2 hours at 5 °C, the cooling water was turned off and the suspension was aged for 60 hours at 20 °C. The resulting suspension was centrifuged and resuspended in distilled, deionized water. This procedure was repeated three times before drying at 120 °C in a laminar air flow hood.

Gibbsite was synthesized by contacting 200 ml (0.1 moles) of the pre-cooled (5 °C) alkoxide stock solution with a 300 ml of water containing 0.015 g NaOH. The mixture was stirred at 5 °C for two hours and then aged for 60 hours at 20 °C before centrifuging, resuspension and drying at 120 °C in a laminar air flow hood.

3.2 RAW MATERIAL CHARACTERIZATION

The dehydroxylation behaviour and transformation sequences of the aluminium hydroxides are considered to be central to the understanding and optimization of the synthesis of β''-Al_2O_3 from these materials.

The aluminium hydroxides were subjected to DTA investigations and were heated to equilibrium (24 hours) at temperatures

ranging from 600 - 1200 °C at 100 °C intervals. This study aimed at characterizing the dehydroxylation behaviour of the materials and determining their reordering sequences.

A common feature of the thermal behaviour of all these materials is that most events involving exothermic or endothermic processes during heating occur below 600 °C. The only detectable thermal event above 600 °C is the transformation to α-alumina which occurs between 1100 and 1200 °C for all materials except diaspore which, as already noted, is the only form of aluminium hydroxide which transforms directly to α-alumina at about 480 °C. All these materials lose the more than 98 per cent of their lattice water below 600 °C.

DTA traces were generated on a Du Pont 1090 thermal analyser. Approximately 0,1 g of the powdered sample was compacted at about 20 MPa to form a pellet of 4 mm diameter and approximately 6 mm thick. The sample was loaded into a platinum sample holder. An identically compacted high purity alumina was used as a reference material. The optimal heating and cooling rate was found to be 5 °C per minute. Two parameters were used to describe the thermal events appearing on the DTA traces. The peak temperature (A) was defined as the maximum/minimum value of thermal event. The onset temperature (B) was defined as the point of intersection of the baseline with the slope at the point of inflection of the thermal event. These two parameters are illustrated in Fig. 3.2.

After heating to equilibrium in a Kanthal furnace, the samples were ground in a agate mortar and pestle together with 2,5 mass per cent silicon XRD standard. Approximately 0,5 g of the powder mixture was mounted on a glass XRD sample holder and X-ray diffractograms were obtained from a Rigaku X-ray diffractometer (Model Geigerflex D.Max III) with a CuKα beam, generated at 40 kV and 25 mA. The samples were all run in the 2θ range (5^0-70^0) with a step-width of $0{,}02^0 2\theta$ at 2 seconds per step.

The thermal analysis and powder X-ray diffraction results are discussed under the respective aluminium hydroxide materials.

3.2.1 **Monohydrates** (Boehmite and Pseudoboehmite)

The X-ray diffraction patterns of the monohydrates are presented in Fig. 3.1. The pseudoboehmite shows broad bands which coincide with the strong reflections of the well-crystallized hydrothermal boehmite. In the case of the pseudoboehmite, the peak position of the 020 reflection is shifted to a lower angle value than the hydrothermal boehmite. This shift in d spacing for the pseudoboehmite confirms the suggestions by Papee, Tertian and Biais (1958) that pseudoboehmite cannot be regarded as a finely divided hydrothermal boehmite. This observed increase in d spacing is due to the accommodation of excess water in the pseudoboehmite lattice.

Figure 3.2 represents the comparative DTA traces of hydrothermal boehmite and pseudoboehmite. Both samples show significant surface water loss as indicated by an endotherm with a peak position at 120 °C. The pseudoboehmite sample shows a larger endotherm associated with the surface water loss than the boehmite sample. This is due to the larger surface area and smaller particle size of the pseudoboehmite sample when compared to the hydrothermal material.

Pseudoboehmite shows a broad dehydroxylation endotherm with an onset temperature of 320 °C and a peak position of 450 °C. An exotherm with an onset temperature of 1200 °C and a peak position of 1220 °C was also noted. Upon cooling, no thermal events were observed confirming the suggestion that the transition aluminas are irreversible reordering sequences.

At 600 °C the transition alumina derived from pseudoboehmite appeared to be a poorly crystalline material as indicated by the broad XRD reflections. The quality of the X-ray data was

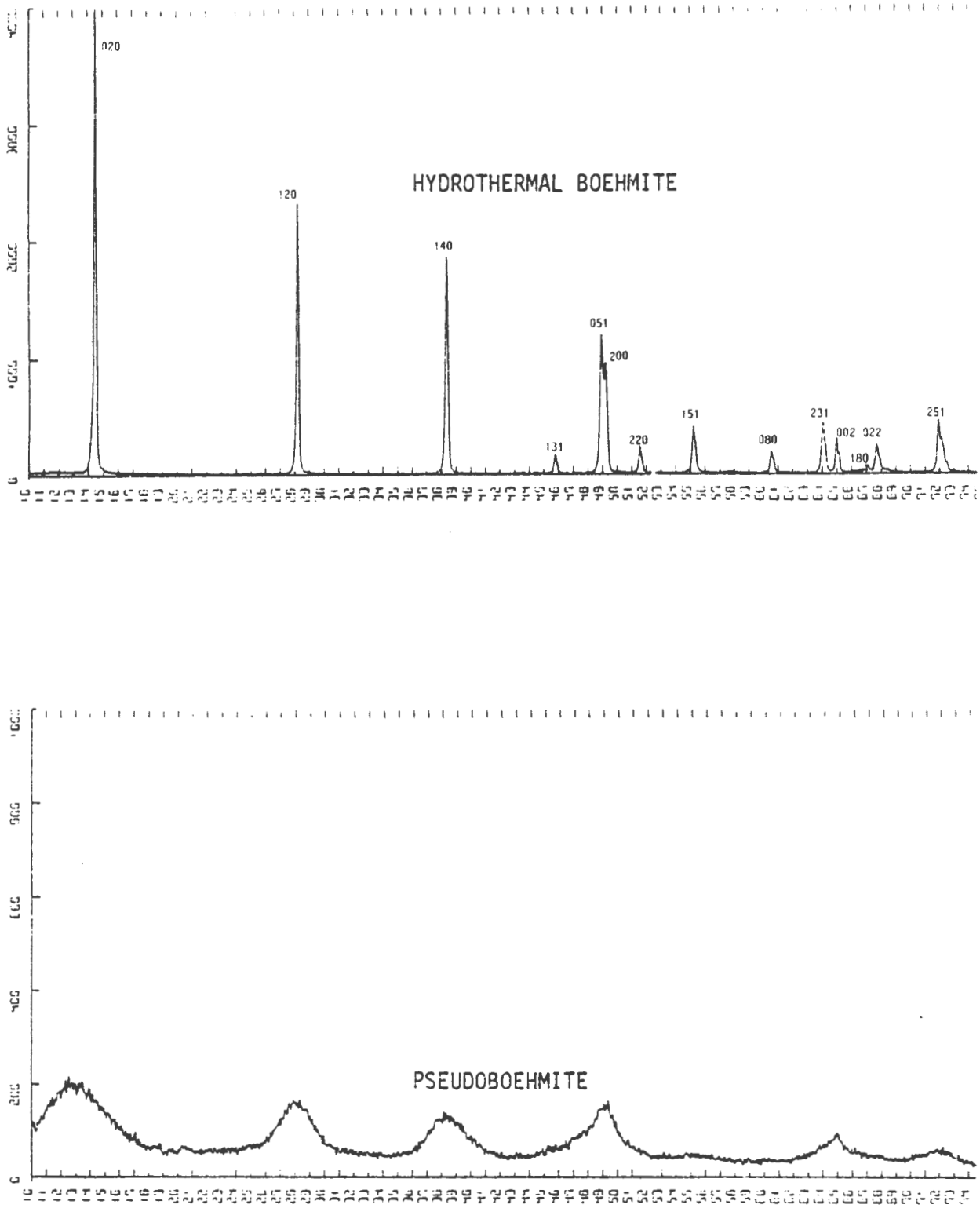

FIGURE 3.1: Diffraction traces of monohydrates

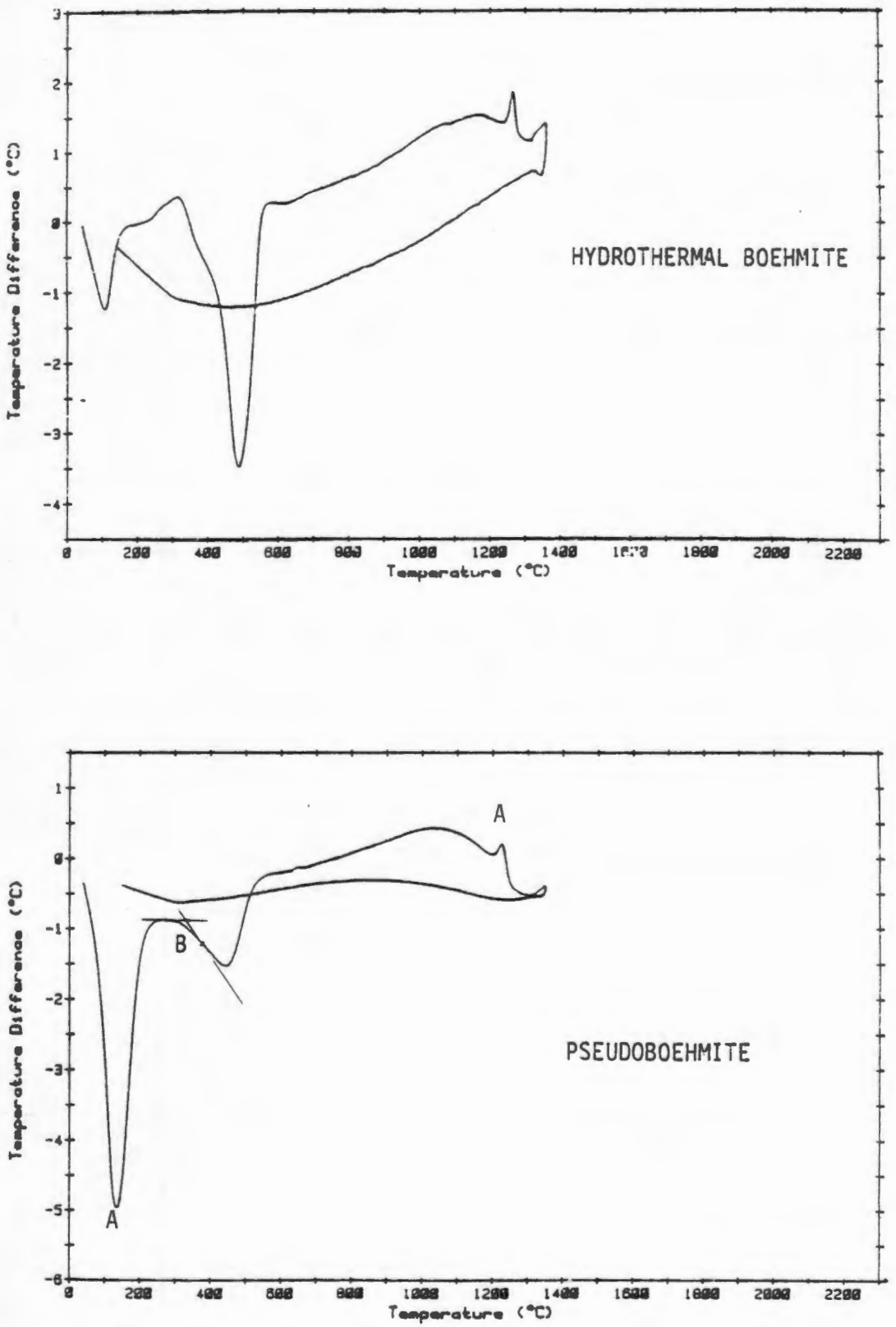

FIGURE 3.2: Comparative DTA traces of monohydrate materials

very poor and it was difficult to index the transition aluminas.

The patterns of pseudoboehmite heated to 900 °C could be indexed as η-Al_2O_3 or poorly crystalline, highly disordered γ-Al_2O_3. At 900 °C the material contained traces of α-Al_2O_3 and some θ-Al_2O_3. After 24 hours at 1 000 °C the material had completely converted to α-Al_2O_3.

Hydrothermal boehmite showed a large dehydroxylation endotherm with an onset temperature of 430 °C and a peak position of 500 °C. A sharp exotherm with an onset temperature of 1240 °C and a peak position of 1270 °C denotes the shear transformation of the cubic transition alumina to hexagonally close-packed α-Al_2O_3. Upon cooling, no thermal events were observed.

Hydrothermal boehmite formed γ-Al_2O_3 when heated to equilibrium at 600 °C. Around 700 °C traces of δ-Al_2O_3 appeared while at 800 °C the majority of the material had converted to δ-Al_2O_3 with traces of γ alumina remaining. At 900 - 1000 °C the material contained mostly δ-Al_2O_3 and θ-Al_2O_3. The identification of the phases by XRD at these temperatures was complicated by the diffuse nature of the XRD spectra of the different transition alumina phases. At 1100 °C α-Al_2O_3 appeared while traces of θ-Al_2O_3 were still present. At 1200 °C all the material had converted to α-Al_2O_3.

The differences in dehydroxylation temperature and temperature of transformation to α-Al_2O_3 of boehmite and pseudoboehmite can be explained in terms of the relative ordering of these materials and their dehydroxylation products. When examining the X-ray diffraction traces of these materials (Fig. 3.1) a difference in the peak position of the 020 reflection as well as broadening of the peaks are noted. This increase in d spacing and peak broadening for pseudoboehmite

indicates lack of complete registry between layers and increased accommodation of water between the $[Al_2(OH)_6]_n$ layers as suggested by Tertian and Papeé (1958). The disorder in the accommodation of protons and OH groups implies lower bond strengths of the protons and the OH groups and hence a lower dehdroxylation temperature, as was observed. The increased d-spacing for pseudoboehmite also implies less resistance to diffusion for the protons and water, resulting in a lowering of the temperature of the dehydroxylation endotherm.

The lower onset temperature and smaller intensity of the pseudoboehmite exotherm shows that less energy is required to convert the material to α-Al_2O_3. The lower energy requirement for this shear transformation can be explained by suggesting that the pseudoboehmite dehydroxylation product has smaller domains of order than the boehmite dehydroxylation product. The domains of order in the dehydroxylation products of boehmite and pseudoboehmite are illustrated by TEM micrographs which are presented in Fig. 3.3. These micrographs show hydrothermal boehmite to contain substantial domains of long range order while pseudoboehmite consists of a fine fibrous network of particles.

Figure 3.4 shows the comparative thermogravimetric traces of boehmite and pseudoboehmite materials. The gradual mass loss over a wide temperature range in the case of pseudoboehmite material indicates the greater mobility of the lattice water in this material and the lower diffusion resistance caused by the smaller crystallite domain size and greater disorder.

3.2.2 Trihydrates (Bayerite, Gibbsite)

The X-ray diffraction patterns of the trihydrates are presented in Fig. 3.5. Both traces could be indexed as single phase gibbsite or bayerite materials.

TRANSITION ALUMINA
DERIVED FROM BOEHMITE

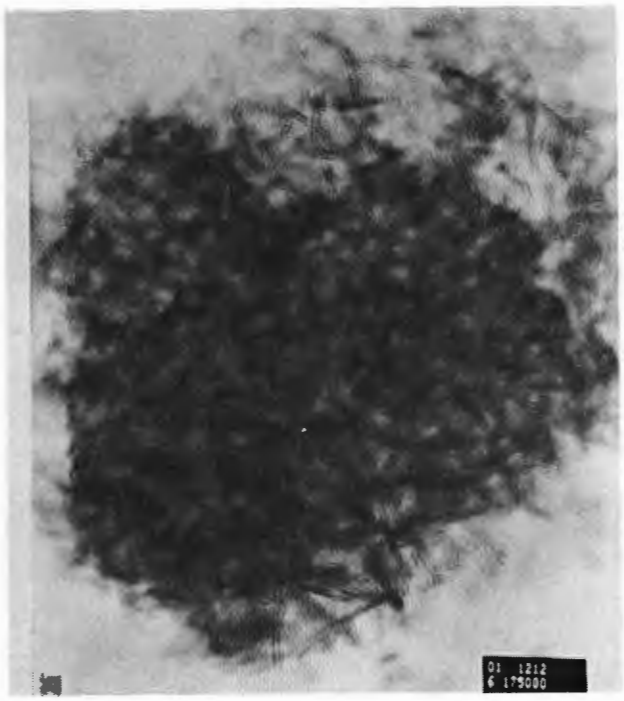

TRANSITION ALUMINA DERIVED
DERIVED FROM PSEUDOBOEHMITE

FIGURE 3.3: TEM photographs of the hydroxylation products of boehmite and pseudoboehmite

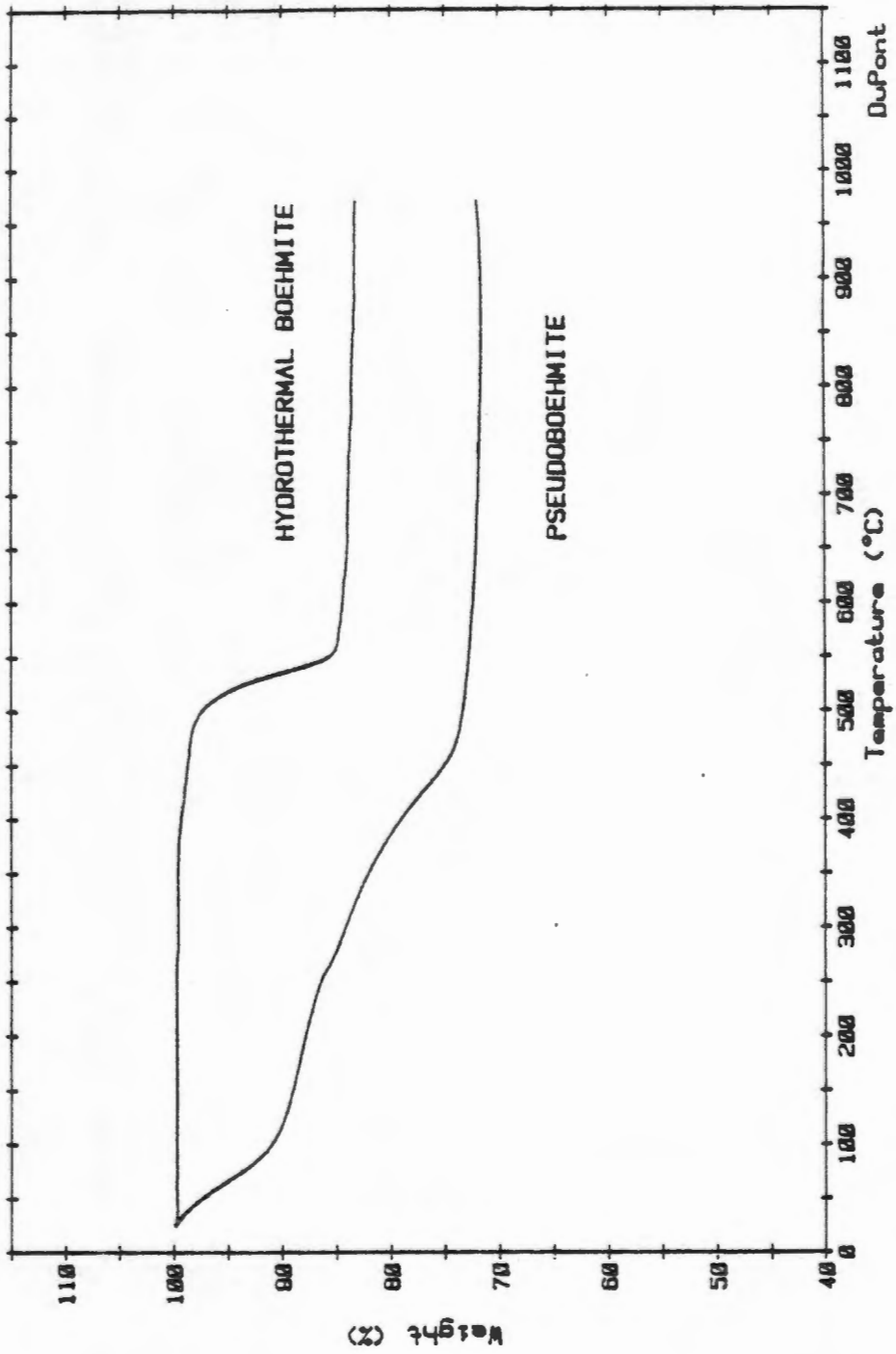

FIGURE 3.4: Comparative TGA traces of monohydrate materials

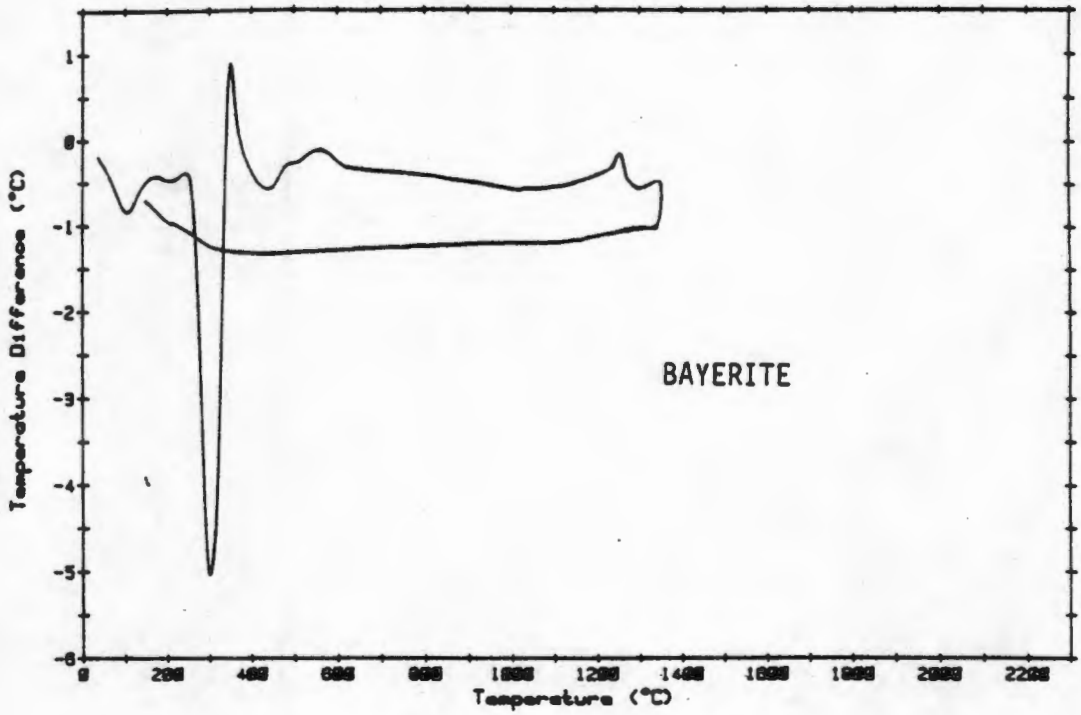

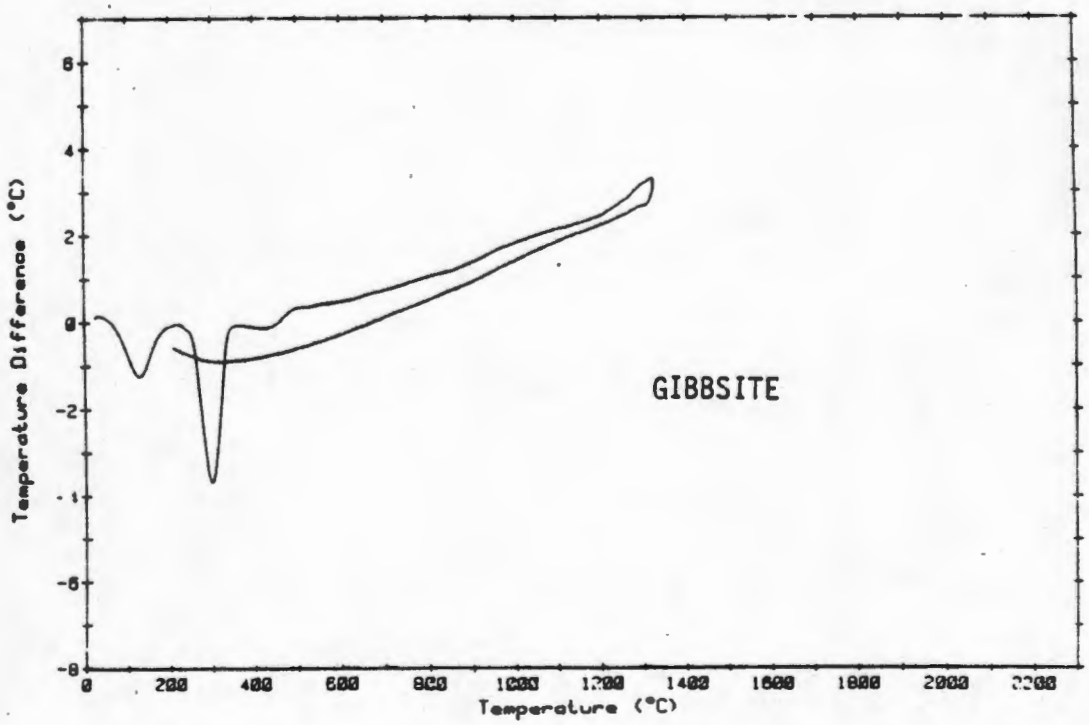

FIGURE 3.5: DTA traces of the trihydrates

Figure 3.6 represents the DTA traces of the synthetic bayerite and gibbsite. Both samples show surface water loss as indicated by an endotherm with a peak position of ~120 °C.

Gibbsite shows a dehydroxylation endotherm with an onset temperature of 220 °C and a peak position of 300 °C. A smaller endotherm with an onset temperature of 350 °C and a peak position of 450 °C is present. No further thermal events are observed in the subsequent heating to 1300 °C and cooling to 100 °C.

Bayerite shows a small endotherm with an onset temperature of 190 °C and a peak position of 220 °C followed by a major dehydroxylation endotherm with an onset temperature of 240 °C and a peak position of 300 °C. Another endotherm is noted at 450 °C. The transformation of γ-Al_2O_3 to α-Al_2O_3 is denoted by an exotherm with and onset temperature of 1220 °C and a peak position of 1250 °C. No thermal events are noted upon cooling of the bayerite.

Two features emerge from the thermograms of the trihydrate materials. In the case of bayerite, a small endotherm is observed prior to the main dehydroxylation event while the gibbsite dehydroxylation endotherm is slightly broadened. These phenomena can be attributed to the formation of boehmite by hydrothermal conditions set up during thermal analysis inside larger trihydrate crystals by retarded diffusion of water out of larger grains. This effect, caused by localized regions of increased steam pressure in the grains is referred to as micro-autoclaving. The formation of small amounts of boehmite from bayerite and gibbsite was confirmed by XRD analysis of trihydrates treated at 300 °C for 30 minutes. The product contained transition alumina and traces of boehmite. The boehmite which is formed by microautoclaving decomposes as the sample is heated. The endotherms with a

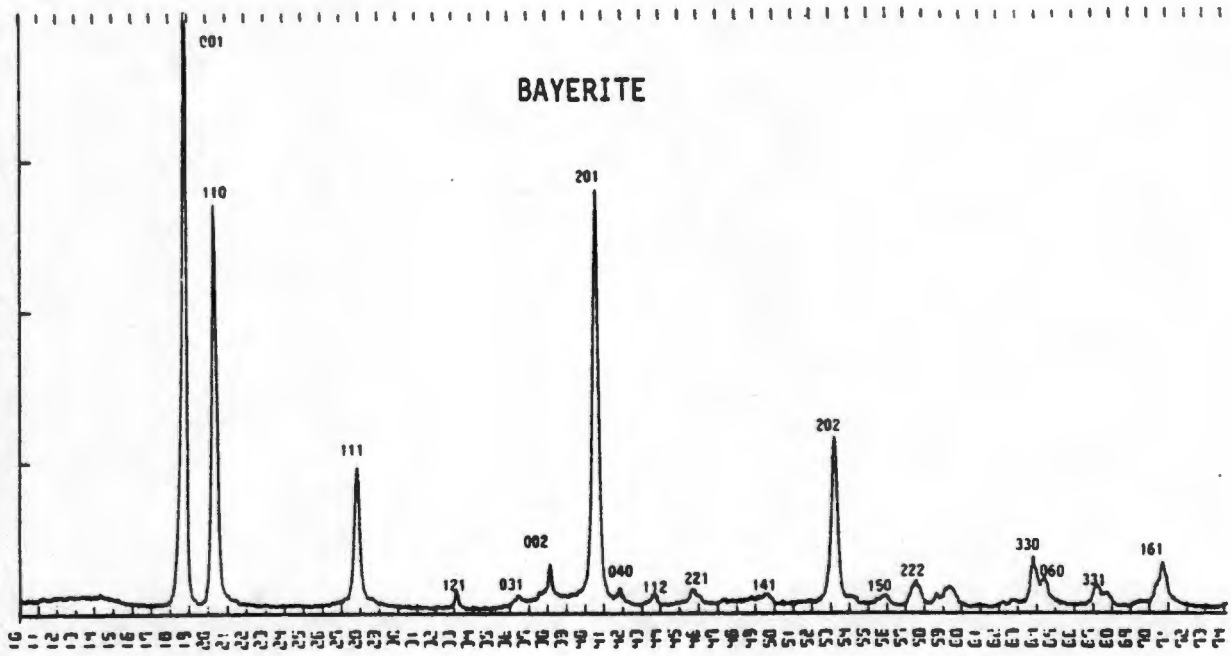

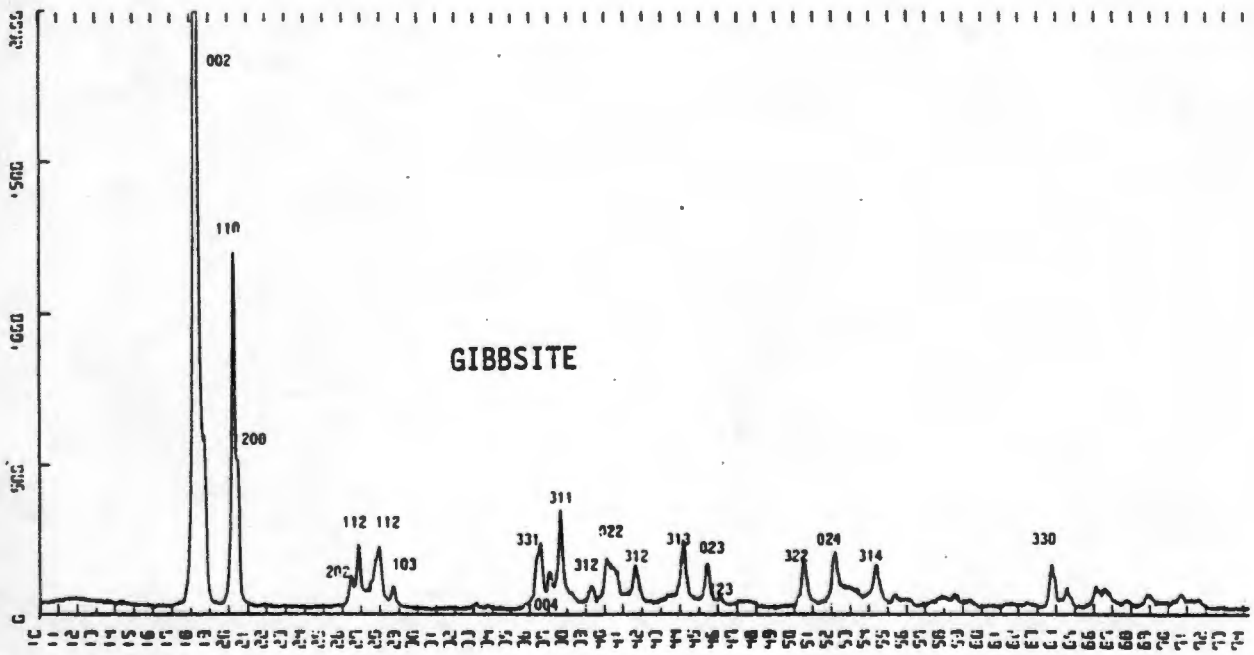

FIGURE 3.6: XRD patterns of the trihydrates

peak position of 450 °C are evidence of boehmite decomposition. This phenomena was previously observed and reported by Goton (1955).

While bayerite shows a definite exothermic transition to α-Al_2O_3, the gibbsite material which contains small amounts of sodium in the lattice, shows no visible thermal event indicating a transition to α-Al_2O_3 at 1300 °C. It appears as if the trace amount of sodium inside the lattice retards the transformation of the transition alumina to α-Al_2O_3. XRD investigations of the system indicated that the transformation from the transition alumina to α-Al_2O_3 was much retarded in the case of gibbsite. A precondition for the retardation is the inclusion of the sodium in the lattice during the synthesis of the hydroxide material. Small amounts of free sodium do not substantially influence the kinetics or temperature of the transformation of the transition alumina to α-Al_2O_3.

The reordering sequences of bayerite and gibbsite were reconstructed from the X-ray diffraction results on equilibrium heated specimens.

After heating to equilibrium at 600 °C, bayerite produced η-Al_2O_3, similar to the dehydroxylation product of hydrothermal boehmite. At 800 °C, θ-Al_2O_3 was detected. α-Al_2O_3 was detected at 900 °C but the material was only fully converted to α-Al_2O_3 by 1200 °C. The DTA (Fig. 3.5) trace of the material showed no thermal events associated with the reordering sequences of the transition alumina but the onset of an exothermic peak was noted at 1250 °C. This exothermic peak was associated with the transition of $\theta \rightarrow \alpha$-$Al_2O_3$. This temperature was found to be considerably higher than the transition temperature for hydrothermal boehmite.

Gibbsite always contains small amounts of sodium which influenced the reordering sequence. At 600 °C the material con-

sisted of a highly disordered η-alumina. The quality of the XRD traces made it difficult to distinguish between the transition aluminas. Between 600 and 800 °C the material could be indexed as either η- or χ-Al_2O_3. χ-Al_2O_3 appeared at 900 °C and was present up to 1150 °C. Trace amounts of α-Al_2O_3 were present at 1000 °C while the bulk of the material had transformed to α-Al_2O_3 by 1200 °C. The sodium in the material had reacted with some of the α-Al_2O_3 to form traces of β-Al_2O_3 which were detected at 1200 °C. The DTA (Fig. 3.6) trace showed no thermal events between 600 °C and 1400 °C. No exotherm corresponding to the formation of α-Al_2O_3 from the χ-Al_2O_3 was detected on the DTA trace. The observed reordering sequences of the synthetic aluminium hydroxide materials are presented in Table 3.1.

These observations confirm the original work by Stumpf (1950) on transition aluminas.

TABLE 3.2: A summary of the reordering sequences observed for the aluminium hydroxide materials

HYDROTHERMAL BOEHMITE	γ-Al_2O_3	δ-Al_3O_3	θ-Al_2O_3	α-Al_2O_3
PSEUDOBOEHMITE	η-Al_2O_3		θ-Al_2O_3	α-Al_2O_3
BAYERITE	γ-Al_2O_3/η-Al_2O_3	θ-Al_2O_3		α-Al_2O_3
GIBBSITE	χ/CHI-Al_2O_3		χ-Al_2O_3	α-Al_2O_3

CHAPTER 4

This chapter describes the systematic solid state reactions of the synthetic aluminium hydroxide raw materials with lithia and soda. A description of powder preparation and high temperature reaction procedures will be followed by a proposed mechanism for the formation of beta alumina from aluminium hydroxides.

4.1 EXPERIMENTAL METHODS

The five raw materials used in the solid state synthesis of beta alumina are listed in Table 4.1.

TABLE 4.1: Raw materials used in the solid state synthesis of beta alumina.

	Material	Preparative method
Monohydrate	Boehmite	Autoclaved synthetic pseudoboehmite
	Pseudoboehmite	Alkoxide hydrolysis at 80 °C
Trihydrate	Bayerite	Alkoxide hydrolysis at 5 °C
	Gibbsite	Alkoxide hydrolysis at 5 °C containing 100 ppm sodium
Corundum	α-alumina	pseudoboehmite calcined at 1400 °C

Sodium and lithium were added in the form of Li_2CO_3 and Na_2CO_3. Sodium carbonate is hygroscopic and was always dried overnight at 320 °C to ensure accurate batching. Sodium and lithium were added to the hydrate to obtain a composition of 84 mole per cent Al_2O_3, 13 mole per cent Na_2O and 3 mole per cent Li_2O (90,53 mass per cent Al_2O_3, 8,52 mass per cent Na_2O and 0,95 mass per cent Li_2O). This composition was

chosen as it represents the central point of the pure β''-Al_2O_3 phase field in the phase diagram for Na_2O, Li_2O and Al_2O_3 system at 1500 °C reported by Duncan and West (1983).

4.1.1. Powder Preparation

Five powder batches were prepared with the specific aluminium hydroxide plus lithia and soda in the correct stoichiometric proportions.

Each batch was prepared as follows. Approximately 75 g of the aluminium hydroxide precursor was accurately weighed into a teflon beaker. The sodium and lithium carbonates were added in the correct stoichiometric proportions. A slurry was made by adding 100 ml of distilled water to the teflon beaker and lastly, 300 g of ZrO_2 grinding media (1 - 2 mm diameter spheres) was added to the slurry. The teflon beaker containing the slurry and grinding media was fitted to an attritor mill and the slurry was milled at 850 rpm for 2 hours. After milling, the slurry was separated from the grinding media by sieving. The slurry was well dispersed and stable. No segregation of the particles and the liquid media was observed after 6 hours. The aqueous slurry contained soluble sodium carbonate, sparingly soluble lithium carbonate and the insoluble aluminium hydroxide.

The distribution of the sodium and the lithium in the slurry needs to be preserved during the drying process to ensure a homogeneous reaction mixture. Various slurry drying techniques such as solvent removal by heating, spray-drying and freeze-drying were previously investigated [Van Zyl and Duncan (1986a)]. Solvent removal by heating produced powders with sodium and lithium inhomogeneities because of the difference in solubility of the two salts. Spray-drying produced powders of good homogeneity but poor stoichiometry because of the loss of a certain fraction of the material in the exhaust

gas. Freeze-drying proved to be the most acceptable drying technique as it produced homogeneous powders of controlled stoichiometry. Because of the convenience and reproducibility of freeze-drying, all slurries were dried in this way.

The freeze-drying of the slurry consisted of two steps. The first step involved the rapid freezing of the slurry. The slurry was injected into a flask containing liquid nitrogen using a syringe with a bore of 0,5 mm. The stream of slurry broke up into droplets with a diameter of approximately 2 mm which froze rapidly in the liquid nitrogen ensuring compositional homogeneity of the final product. The second step involved the transfer of the frozen slurry globules together with some liquid nitrogen into a pyrex sample holder, which was subsequently fitted to a commercial freeze-dryer. All freeze-drying was carried out at a vacuum of 0,06 millibar and a condenser temperature of -50 °C. Freeze-drying produces free flowing, homogeneous, unagglomerated powders suitable for reaction and sintering.

Five batches of powder were produced using the above preparative techniques. All powders were stored under argon to prevent adsorbtion of water by the hygroscopic salts. The yield was calculated and in each case the figure exceeded 98 per cent.

4.1.2 Solid State Reaction and Characterization of Precursor Powders

The reaction pathways of the aluminium hydroxides in the presence of the alkali salts, were investigated by the solid state reaction of the precursor powders at temperatures ranging from 600 °C to 1200 °C in 100 °C intervals, and at 1600 °C.

The reaction mixtures were subjected to DTA investigations and the equilibrium reaction products at different temperatures were investigated by X-ray diffraction techniques. These techniques are fully described in Section 3.2.

Prior to reaction, the samples were compacted at 20 MPa into cylindrical discs with a diameter of about 10 mm and a thickness of about 5 mm. The compacted samples were encapsulated in platinum foil to prevent soda loss to the furnace environment during reaction. The platinum-encapsulated samples were placed in an alumina crucible and reacted in a low thermal-mass Super Kanthal furnace. In all cases the heating and cooling rates were 300 °C per hour, which corresponded to the DTA heating rate of 5 °C per minute. Samples were reacted to equilibrium (approximately 24 hours) at temperatures ranging from 600 - 1200 °C at 100 °C intervals.

4.2 RESULTS

The results of the DTA and X-ray diffraction investigations of each material are discussed separately.

4.2.1 α-Al_2O_3

A reaction mixture of α-Al_2O_3, Na_2CO_3 and Li_2CO_3 was prepared and reacted under the conditions described earlier. The α-Al_2O_3 containing a reaction mixture was used to contrast the known crystallization pathway [Bugden and Duncan (1979)] with that of the aluminium hydroxide precursors.

The DTA and TGA traces for the reaction mixture α-Al_2O_3, Na_2CO_3 and Li_2CO_3 are presented in Fig. 4.1. A strong endotherm with a peak position of 100 °C indicates a surface water loss of approximately 2%. A small endotherm with a peak position of 500 °C indicates the decomposition of Li_2CO_3. The TGA trace confirms that this decomposition takes place over a temperature range 450 - 650 °C. A broad endotherm with a peak position of approximately 650 °C denotes the decomposition of Na_2CO_3. The TGA trace indicates that the Na_2CO_3 decomposition occurs over the temperature 600 - 750 °C. After this temperature no significant further mass loss was detected.

The final thermal event in the heating of the reaction mixture is an endotherm with a peak position of 780 °C. As no significant mass loss is associated with this event, it is assumed to be due to the partial transformation of α-Al_2O_3 to γ-$NaAlO_2$, a intermediate product in the formation of beta alumina. In this reconstructive transformation of the α-Al_2O_3 oxygen sublattice the hexagonal close-packed structure is changed to a cubic close packed oxygen sublattice. Upon cooling, no thermal events are detected.

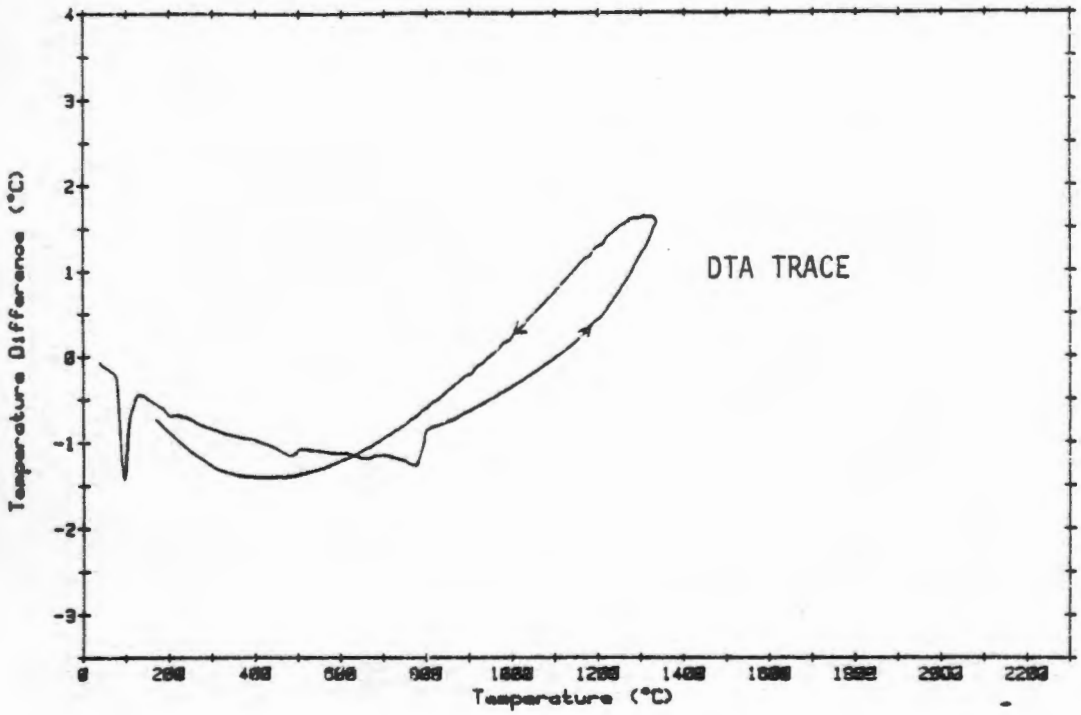

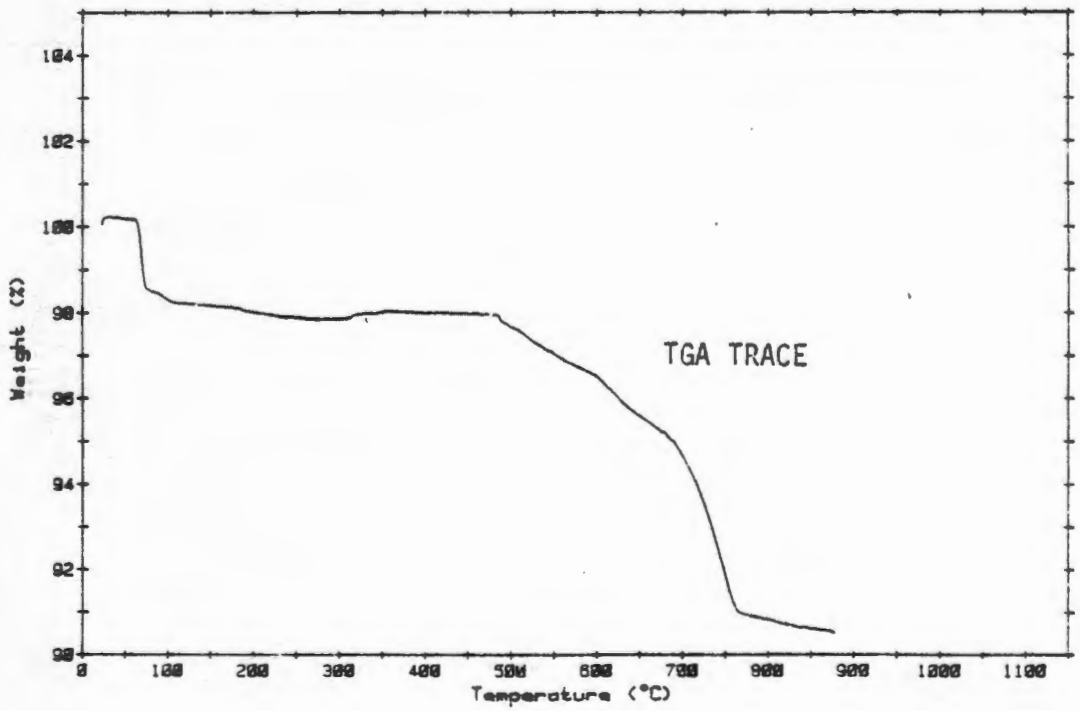

FIGURE 4.1: DTA/TGA traces of α-Al_2O_3, Li_2CO_3, Na_2CO_3 reaction mixture

The results of the equlibrium solid state reaction at 600 °C showed that some of the α-alumina had converted to sodium aluminate. The high temperature γ-$NaAlO_2$ phase was represented at room temperature as ρ-$NaAlO_2.6H_2O$ instead of the expected β-$NaAlO_2$ low temperature phase. The presence of ρ-$NaAlO_2.6H_2O$ is explained by the high surface area of the reaction products which are readily hydrated by moisture upon cooling. This phase was first reported by Elliot and Huggins (1975). The appearance of β-$NaAlO_2$ at higher reaction temperatures is explained by the decrease in the surface area of the reaction product resulting from grain growth. Figure 4.2 illustrates this observation.

The amount of sodium aluminate increased with reaction temperature. By 1100 °C no α-Al_2O_3, or any form of $NaAlO_2$ could be detected by XRD as all the material had been converted to a two-phase mixture of β-Al_2O_3 and β"-Al_2O_3 with the β-Al_2O_3 phase predominating. At 1200 °C the phase assemblage was essentially similar to the 1100 °C product, except that the reflections were sharper, indicating a degree of crystal growth.

After ten minutes at 1 600 °C, with a heating and cooling rate of 300 °C per hour the sample contained a mixture of β-Al_2O_3 and β"-Al_2O_3 with the β"-Al_2O_3 phase predominating. The phase development of the reaction products derived from α-Al_2O_3 is presented in Fig. 4.2.

4.2.2 Hydrothermal boehmite

The DTA and TGA traces of the hydrothermal boehmite, Na_2CO_3 and Li_2CO_3 reaction mixture are presented in Fig. 4.3. An endothermal peak at 100 °C indicates surface water loss. In addition to the characteristic strong endothermic decomposition of boehmite with a peak position of about 450 °C, two weaker endotherms are observed at 300 and 400 °C respective-

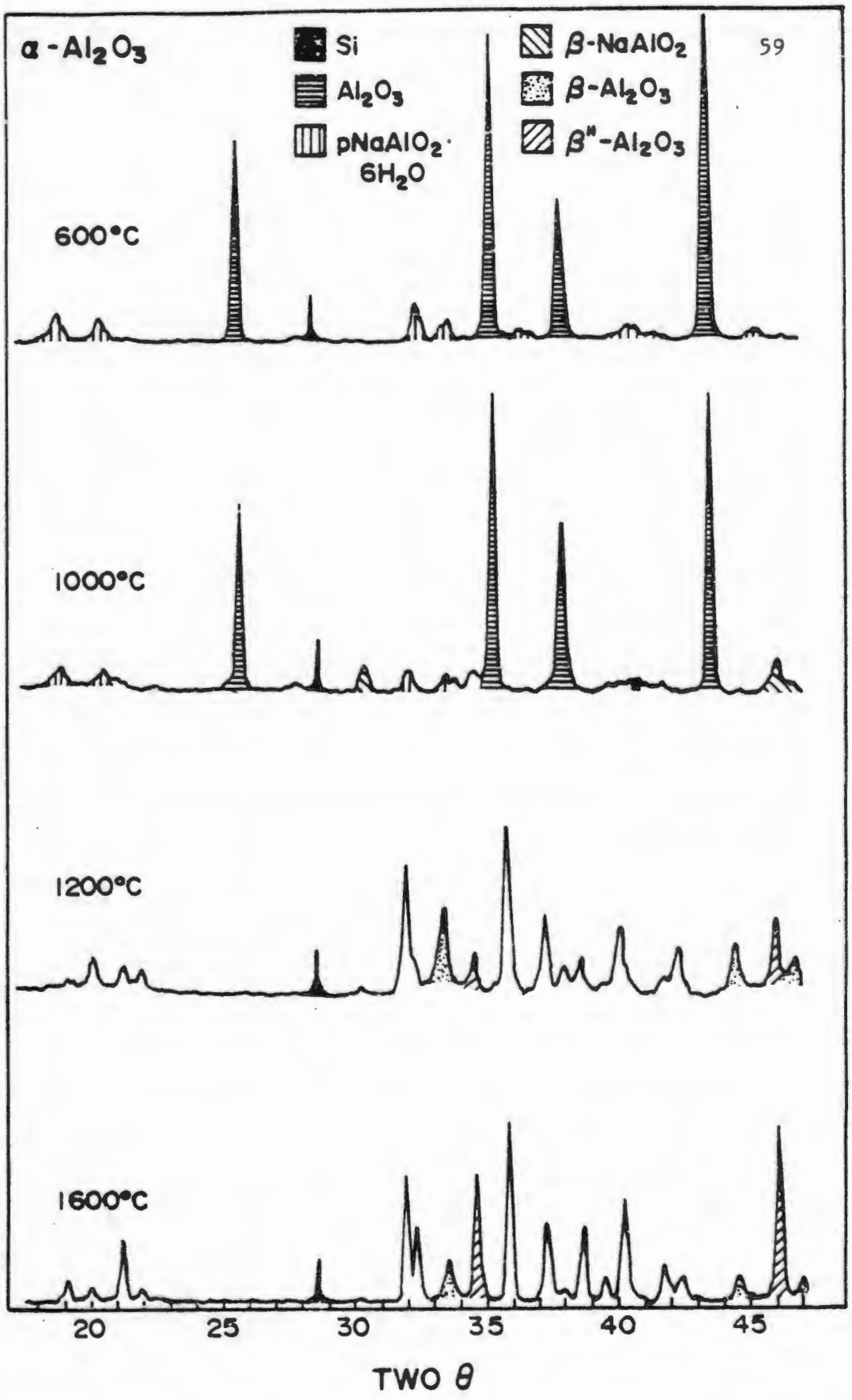

FIGURE 4.2: Phase development beta alumina reaction products derived from α-Al_2O_3

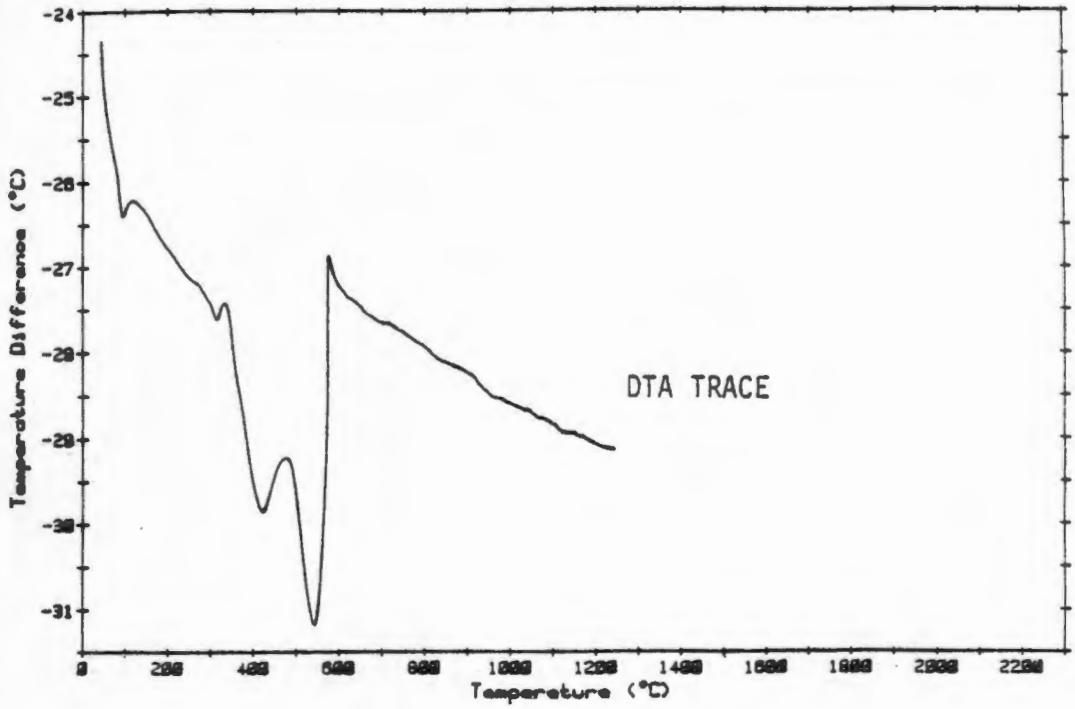

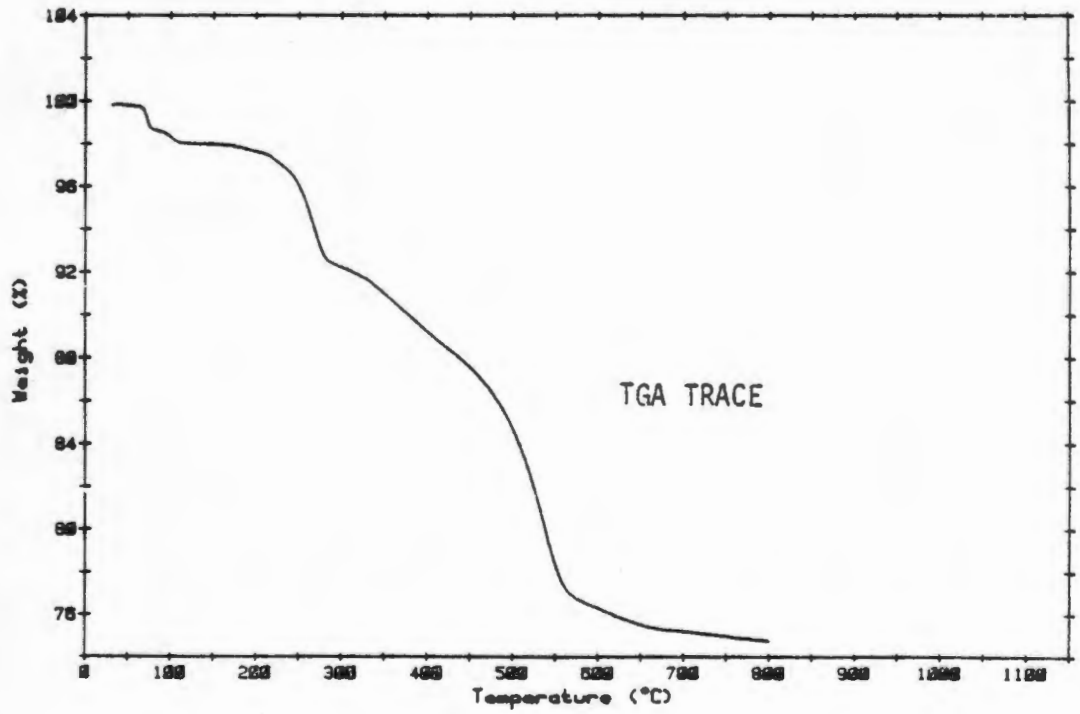

FIGURE 4.3: A DTA and TGA trace of the boehmite reaction mixture

ly. These two endotherms are absent in reaction sequence of α-Al_2O_3 reaction mixture (Fig. 4.1), and can be explained as follows. The initial steam release from the aluminium hydroxide decomposition causes the following reactions to take place:

$$Li_2CO_3 + H_2O \rightarrow 2LiOH + CO_2 \quad \text{and}$$
$$Na_2CO_3 + H_2O \rightarrow 2NaOH + CO_2$$

It is proposed that the endotherm at 300 °C represents the Li_2CO_3 steam reaction while the endotherm 400 °C represents the Na_2CO_3 steam reaction. Therefore, the Na_2CO_3 decomposition peak observed in the α-Al_2O_3 reaction mixture at about 650 °C is absent. The absence of the lithium carbonate decomposition endotherm cannot be confirmed because of the major dehydroxylation event at 500 °C. The TGA trace confirms the suggestion of steam solvation of the carbonate salts indicating that the majority of mass loss occurs below 650 °C.

In the other aluminium hydroxide reaction mixtures, the same steam solvation reaction of the carbonate salts is assumed to occur.

After 600 °C, no detectable thermal events were observed for the boehmite reaction mixture. This would seem to indicate that the oxygen sublattice does not undergo a reconstructive transformation as observed in the α-Al_2O_3 reaction mixture.

The boehmite-containing reaction mixture at 600 °C showed no traces of sodium aluminate by XRD. In most respects the 600 °C XRD pattern was similar to that of γ-Al_2O_3, the dehydroxylation product of the pure boehmite material. The pattern of the sodium- and lithium-containing material had an additional peak in the region of 32° 2θ while the 400 and 440 spinel peaks were shifted to lower angle values, indicating an increased d-spacing for these reflections. As the tempera-

ture was increased to 900 °C, the broad peak in region of 32° 2θ became progressively sharper. Between 600 and 900 °C no new phases appeared. The additional peak at 32° 2θ does not correspond to any of the known sodium aluminate phases. At 1000 °C, this peak developed into the 110 and 111 β"-Al_2O_3 reflections. At 1200 °C only β"-Al_2O_3 was observed after 24 hours of reaction time. After 10 minutes at 1600 °C with a heating and cooling rate of 300 °C per hour, the material was a well-crystallized, single phase β"-Al_2O_3.

During the solid state reaction of boehmite with the alkali salts, no β-Al_2O_3 or sodium aluminate was observed as intermediate products. The phase development of single phase β"-Al_2O_3 from boehmite is shown in Fig. 4.4.

4.2.3 Pseudoboehmite

The DTA trace of relatively high surface area pseudoboehmite reaction mixture, Fig. 4.5, showed an endotherm just above 100 °C corresponding to loss of adsorbed surface water. The onset temperature of the dehydroxylation process occurred at 350 °C. The dehydroxylation endotherm is broadened and is completed by 500 °C. In addition to the standard endothermic peaks for the pseudoboehmite, an additional peak with an onset temperature of 230 °C was observed. This broad peak can be ascribed to the reaction of the sodium and lithium carbonate salts with steam as described earlier. The change in the position and shape of these carbonate reaction peaks compared to the hydrothermal boehmite system, can be ascribed to lower temperature crystal water loss of the pseudoboehmite material (see Fig. 3.4).

The exothermic event with peak temperature of 1150 °C is interpreted as some unreacted disordered transition alumina transforming to α-Al_2O_3. However, an XRD pattern of the DTA product after heating to 1250 °C at 5 °C per minute reveals

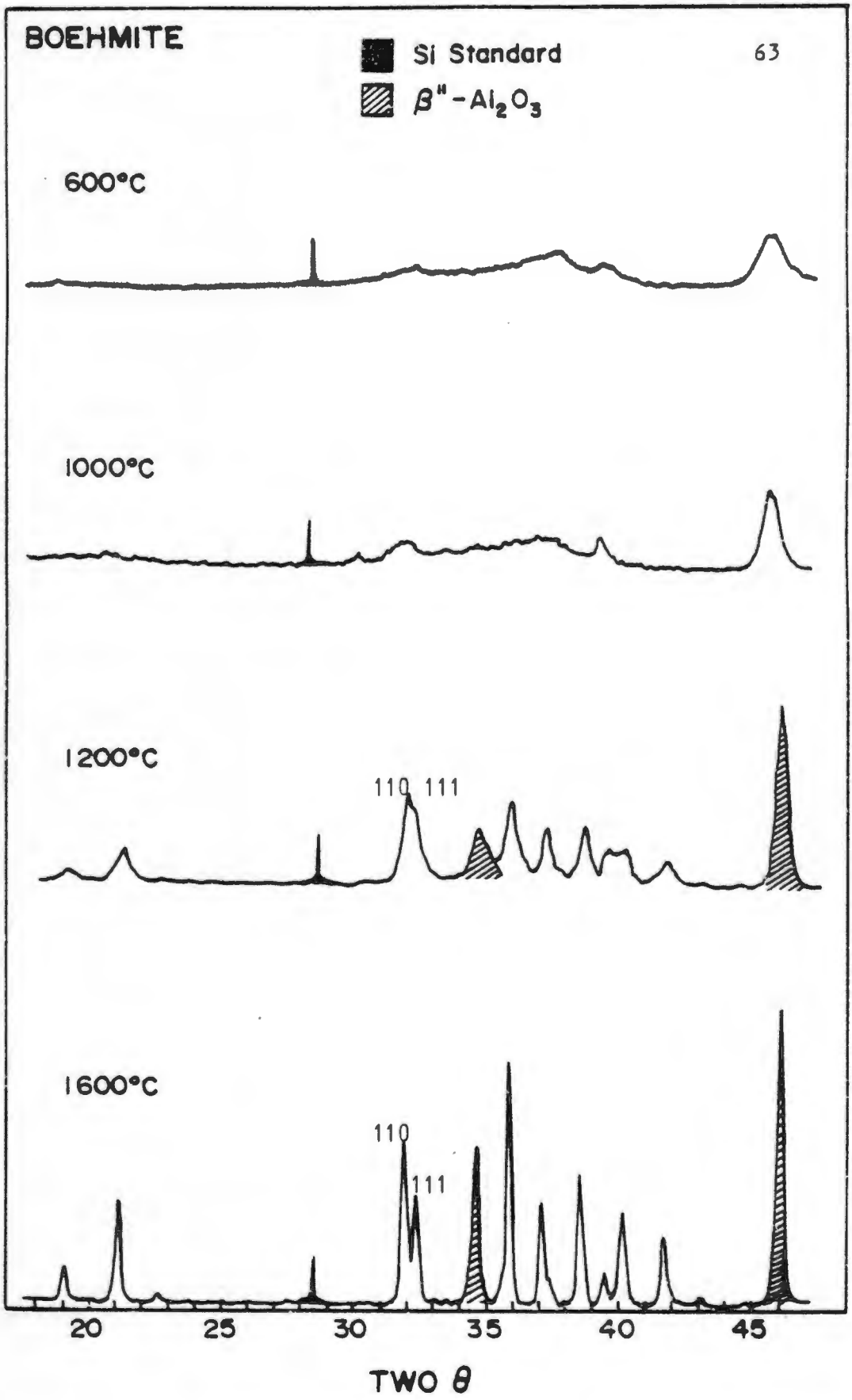

FIGURE 4.4: Phase development of single phase β''-Al_2O_3 derived from hydrothermal boehmite

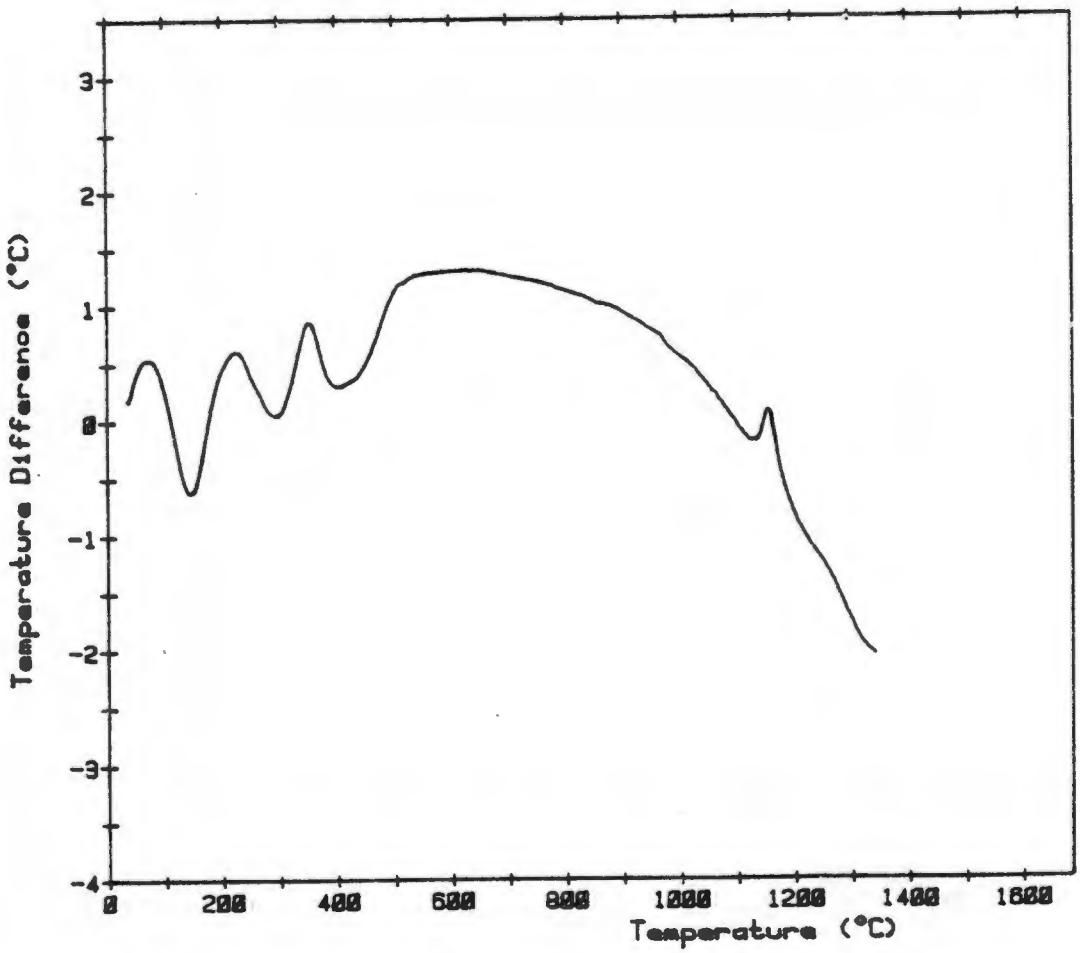

FIGURE 4.5: DTA trace of pseudoboehmite reaction mixture

no α-Al_2O_3. This implies that the α-Al_2O_3 had subsequently reacted with the soda to form a beta alumina product.

After an equilibrium solid state reaction of pseudoboehmite with sodium and lithium carbonate at 600 °C, the reaction product appeared to be virtually amorphous, containing only two broad reflections in the 2θ region of 44-48° and 34-38°. These two reflections remained broad up to 900 °C, although there was some sharpening of the peaks indicating an ordering of the structures as the temperature was increased.

Two unidentified broad reflections appeared in the 2θ regions of 32 and 37° but the quality of the X-ray data was too poor

to index these reflections. At 1000 °C a product appeared which had a mixture of sharp reflections and broad bands. The sharp reflections could be indexed as peaks common to both the β-Al_2O_3 and β"-Al_2O_3 structures while the broad bands occurred in these regions where the unique, characteristic β-Al_2O_3 and β"-Al_2O_3 peaks are located. This phenomena has been described previously by Morgan (1976) and the reaction product is assumed to be an intergrown polytype of β-Al_2O_3 and β"-Al_2O_3 and will subsequently be referred to as β/β"-Al_2O_3. As the temperature was increased to 1200 °C the peaks common to both β-Al_2O_3 and β"-Al_2O_3 became sharper while the broad peaks characteristic of the intergrown material persisted. Even after 10 minutes at 1600 °C, the intergrown structure persisted. It has been reported by De Jonge (1977) that this structure cannot be changed by temperature treatment below the melting point of the material. The phase development of the beta alumina intergrown product derived from pseudoboehmite is presented in Fig. 4.6.

4.2.4 Bayerite

A DTA trace of the bayerite reaction mixture (Fig. 4.7) indicated the loss of surface water just above 100 °C. The characteristic dehydroxylation endotherm of bayerite with a peak position of 300 °C was very much broadened in the DTA trace of the reaction mixture. The onset temperature for the thermal event was also lowered to 200 °C. As in the case with the reaction mixtures of boehmite and pseudoboehmite, this broadening is ascribed to the dissolution of the carbonate salts by the steam released during heating.

Apart from the small characteristic monohydrate dehydroxylation endotherm at 500 °C (refer Section 3.2), no other thermal events were detected up to 1300 °C. This infers that no reconstructive transformation of the oxygen sublattice of the dehydroxylation product of bayerite takes place during

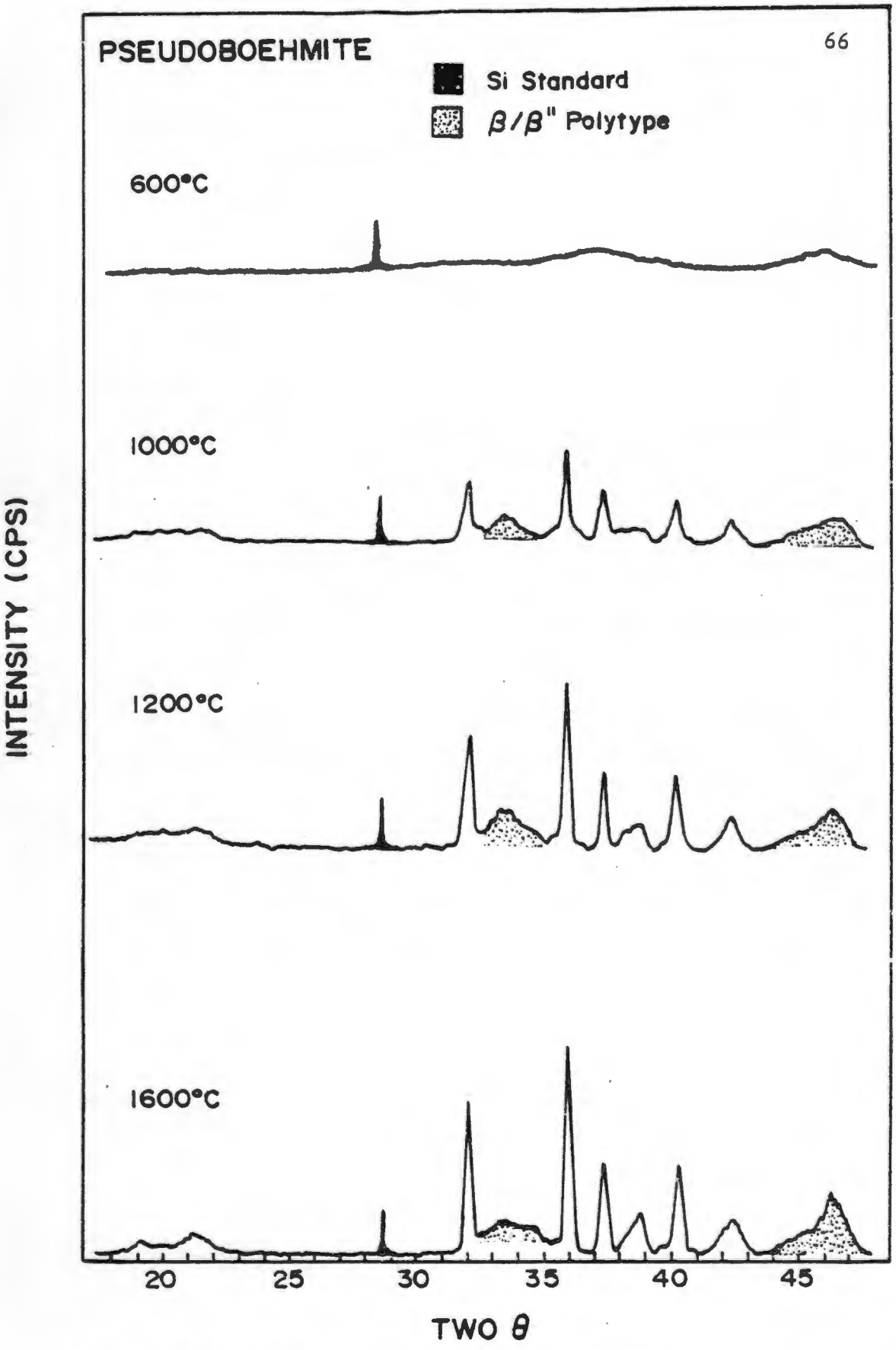

FIGURE 4.6: Phase development of the intergrown beta alumina derived from pseudoboehmite

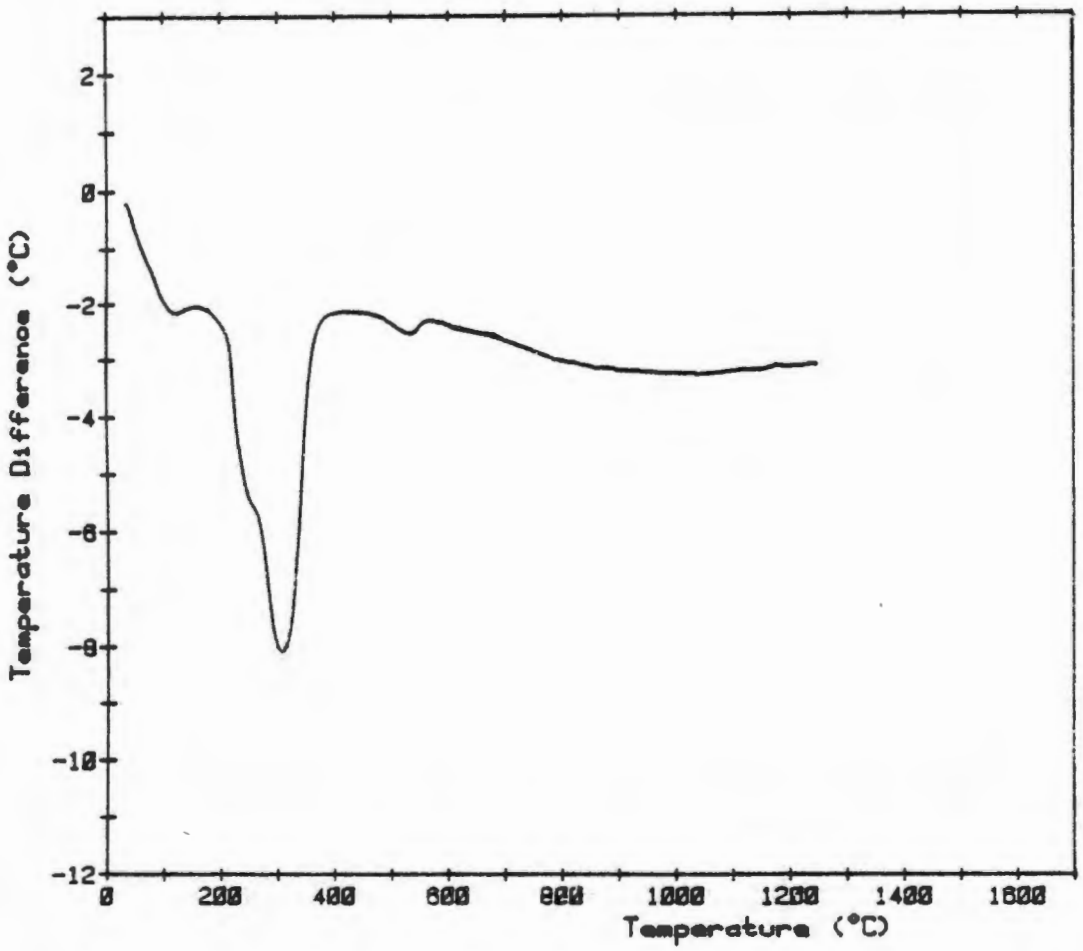

FIGURE 4.7: DTA trace of bayerite reaction mixture

reaction with soda and lithia. This is in contrast to the behaviour of the α-Al_2O_3 reaction mixture.

At 600 °C the bayerite reaction product appeared to be γ-Al_2O_3 with an additional broad reflection in the $2\theta=32^{\circ}$ region. With an increase in temperature, this broad reflection sharpened significantly.

At 900 °C, a reflection not belonging to a sodium aluminate phase appeared. This peak which was well-defined at 1000 °C resolved into the 110 and 111 β"-Al_2O_3 peaks at 1100 °C. At 1200 °C, pure β"-Al_2O_3 was the only phase present while after 10 minutes at 1600 °C, only well-crystallized β"-Al_2O_3 could be detected.

In most respects, the crystallization pathway and products of bayerite were similar to that of hydrothermal boehmite. No sodium aluminate or β-Al_2O_3 were detected as intermediates but in the case of bayerite, the low temperature 'precursor peaks' of β"-Al_2O_3 were slightly better resolved than in the case of the hydrothermal boehmite.

The phase development of single phase β"-Al_2O_3 from bayerite is presented in Fig. 4.8.

4.2.5 Gibbsite

The DTA trace of the gibbsite reaction mixture (Fig. 4.9) showed a broadening of the characteristic major primary dehydroxylation endotherm with an onset temperature of 200 °C. This broadening can be ascribed to the dissolution of the carbonate salts as previously described. Apart from a characteristic monohydrate dehydroxylation endotherm with a peak position onset temperature of 500 °C, no other thermal events occurred while heating the material to 1300 °C. This infers that no reconstructive transformation of the oxygen sublattice of the dehydroxylation product of bayerite occurs when reacted with soda and lithia.

An analysis of the X-ray diffraction data of the reaction products of gibbsite as a function of temperature, showed that a poorly crystalline product similar to η-Al_2O_3 was formed at 600 °C and as the temperature was increased the product became more crystalline. By 900 °C broad peaks occurred in the regions where the intergrown β/β"-Al_2O_3 peaks are located. At 1000 °C, the peaks common to β-Al_2O_3 and β"-Al_2O_3 could be identified, with broad bands occurring in the regions where unique β and β"-Al_2O_3 peaks are located. At 1200 °C the so-called intergrowths, as described for pseudoboehmite, were present and were maintained even after treatment at 1600 °C for 10 minutes. From the X-ray diffraction

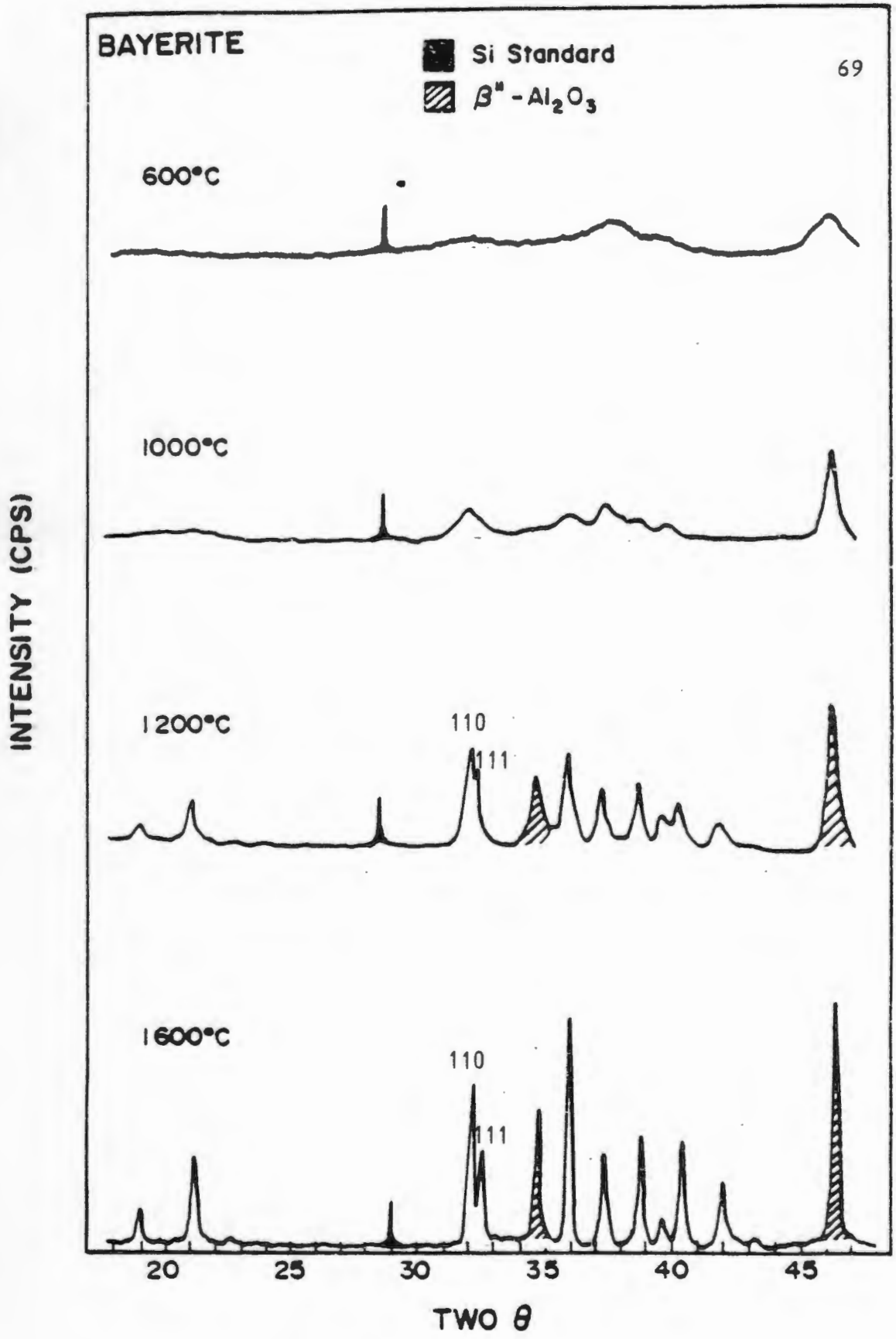

FIGURE 4.8: Phase development of pure β"-Al_2O_3 from bayerite derived material

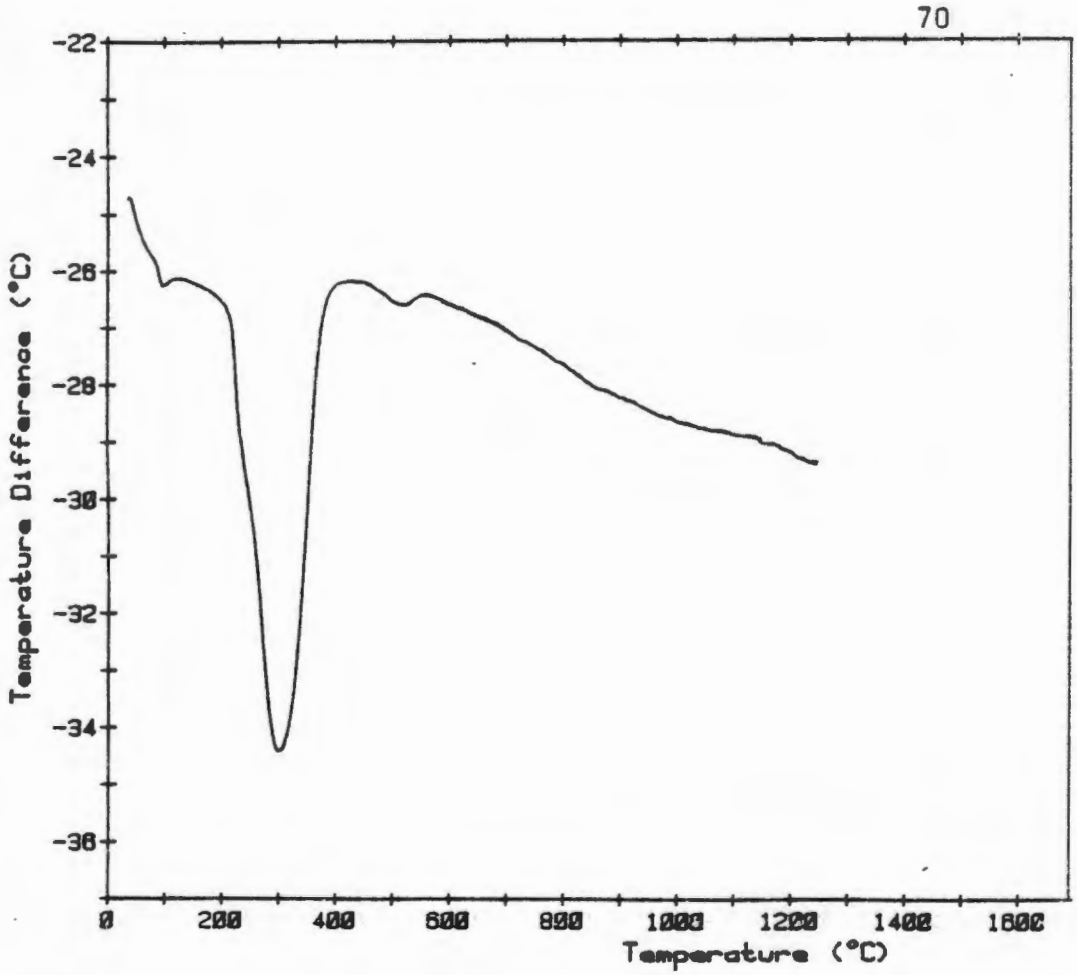

FIGURE 4.9: DTA trace of gibbsite reaction mixture

patterns, however, the intergrowths appear to have a different character to those of the pseudoboehmite. In the case of the gibbsite reaction product, the intergrowth bands are skewed. This indicates that a higher proportion of β''-Al_2O_3 phase is present than in the case of the pseudoboehmite intergrowths.

The phase development of the β/β'' polytype is presented in Fig. 4.10.

A summary of the crystallization pathways and 1200 °C reaction products of the five materials are presented in Table 4.2.

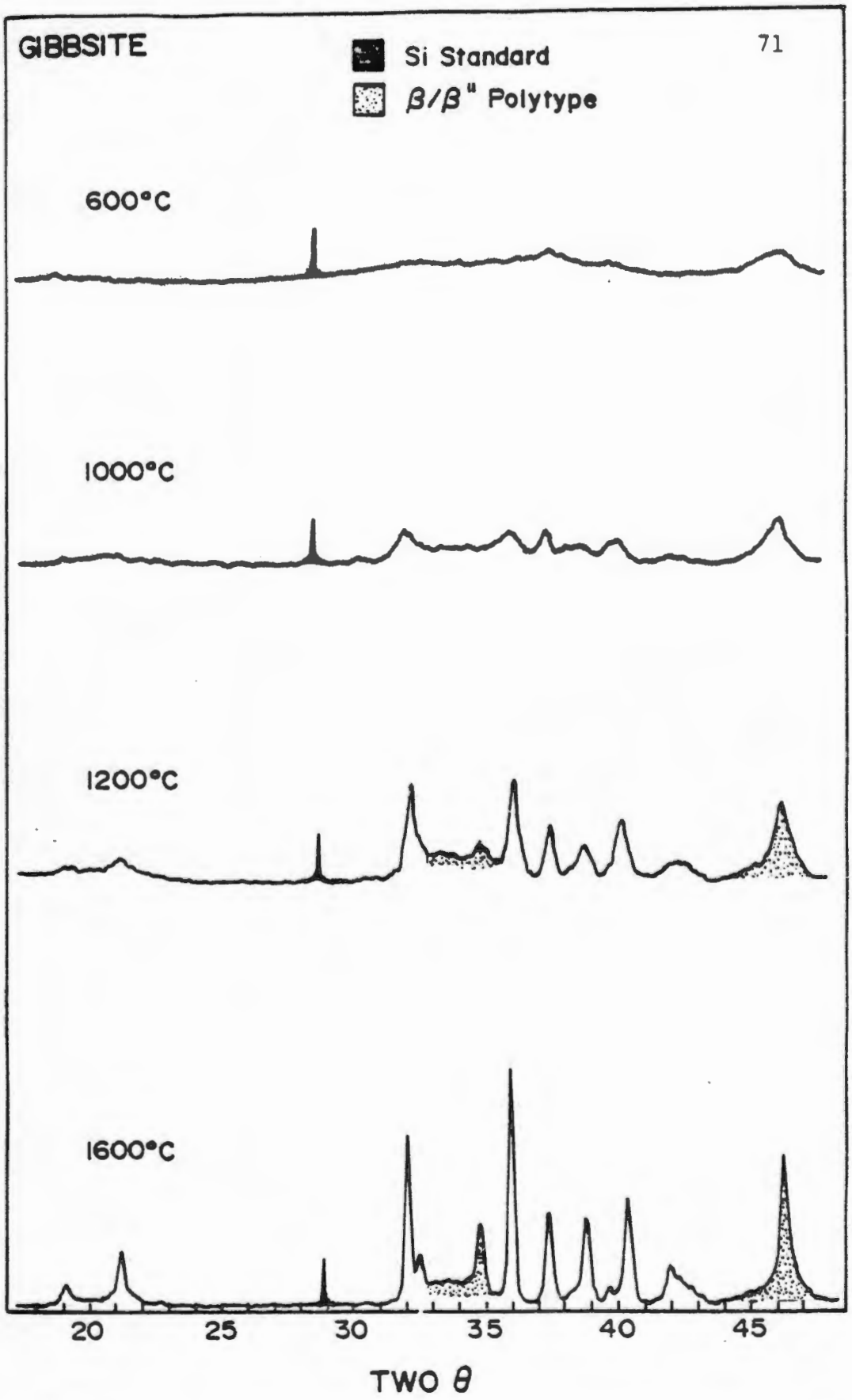

FIGURE 4.10: Phase development of β/β" polytype derived from gibbsite

TABLE 4.2: Crystallization pathways and reaction products of aluminium oxide precursors

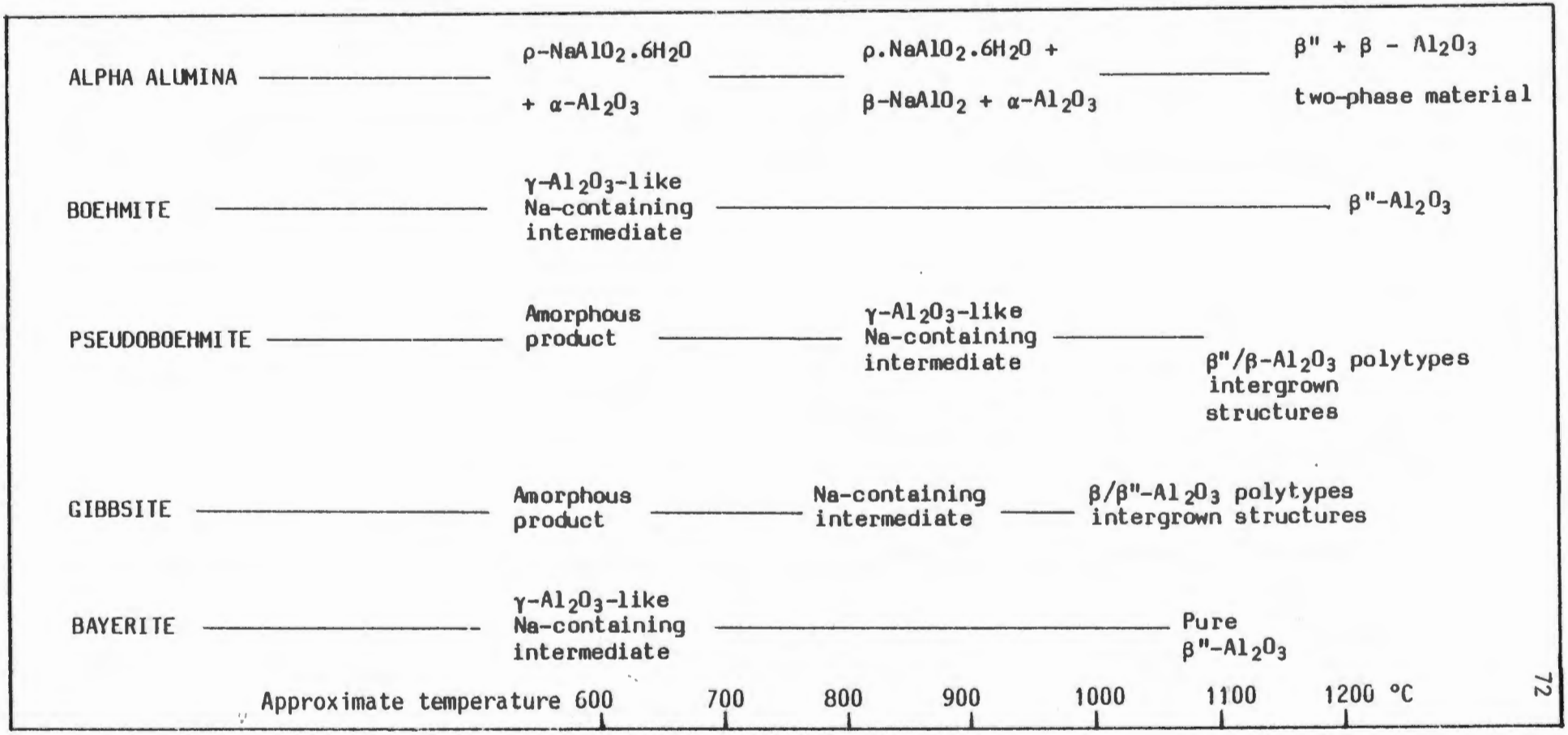

4.3 DISCUSSION

Three distinct types of beta alumina products were identified from the powder X-ray diffraction patterns. These products were derived by distinctly different reaction pathways. The evolution of each type of beta alumina powder product is discussed separately.

4.3.1 Two Phase β-Al_2O_3 plus β''-Al_2O_3 Mixtures

Distinct two-phase mixtures of β plus β''-Al_2O_3 were produced when α-Al_2O_3 was reacted with sodium and lithium salts at 1200 °C. At this temperature the proportion of β''-Al_2O_3 was about 40%. α-Al_2O_3 has a hexagonal close packed oxygen lattice with an [...AB AB AB...] stacking of the oxygen ions. The formation of β and β''-Al_2O_3 from this precursor requires a reconstructive transformation of the oxygen sublattice. The endothermic event at approximately 800 °C is related to the transformation of a portion of the α-Al_2O_3 to γ-$NaAlO_2$ which subsequently reacts with the residual α-Al_2O_3 to form a two-phase mixture of β and β''-Al_2O_3. During these reactions the hexagonal close-packed sublattice of the corundum structure is transformed to a close-packed cubic sublattice.

4.3.2 Pure β''-Al_2O_3 Formation

Hydrothermal boehmite and bayerite produced a single phase, distinctly crystalline β''-Al_2O_3 when reacted with sodium and lithium carbonates at 1200 °C. β''-Al_2O_3 was in both cases produced directly, with no traces of sodium aluminate or β-Al_2O_3 intermediates observed. The direct formation of β''-Al_2O_3 from boehmite was first reported by Duncan (1983) amd Barrow et al. (1986). These authors made an important contribution to the understanding of the direct formation of β''-Al_2O_3 from hydrothermal boehmite. Barrow (1986) pointed out that pure β''-Al_2O_3 is only formed from boehmite which exhibits a long range order of the oxygen sublattice.

The crystal structures of monohydrate hydrothermal boehmite and trihydrate bayerite differ substantially. Bayerite consists of densely packed layers with the aluminium ions arranged on the octahedrally co-ordinated lattice sites. The layers exhibit a hexagonal close-packed sequence with an [...AB AB AB...] oxygen sublattice stacking. Boehmite also has a layered structure in which the Al ions are located in octahedral sites. However, in the case of the boehmite the OH ions are arranged on the outside of the layers and ensure the cohesion of the layers by hydrogen bonding.

The differences in structure are responsible for the different dehydroxylation behaviour observed for these materials. Dehydroxylation of bayerite occurs at an onset temperature of 240 °C while the hydrogen bonds in boehmite require higher temperatures to be broken. This results in an onset temperature of 500 °C for the dehydroxylation of boehmite.

Structural changes in the materials as a result of dehydroxylation were observed in both materials upon heating. Bayerite produced η-Al_2O_3, which has a cubic spinel-like crystal lattice with a lattice constant a = 7,92 Å. γ-Al_2O_3 was formed when boehmite was dehydroxylated. This spinel-like lattice is tetragonally deformed but is in all other cases similar to η-Al_2O_3. The tetragonal deformation of the γ-Al_2O_3 compound is illustrated by the splitting of the 440 and 400 lines of the spinel lattice as indicated in Fig. 4.11. The tetragonal deformation can be explained by the observation of Krishner (1971) who reported that the Al occupation in the boehmite is inherited by the γ-Al_2O_3. Consequently the aluminium ions occupy octahedral sites not usually occupied in spinel structures.

The cubic η-Al_2O_3 formed by the dehydroxylation of bayerite, does not retain the octahedral occupation of the aluminium, resulting in the cubic spinel lattice.

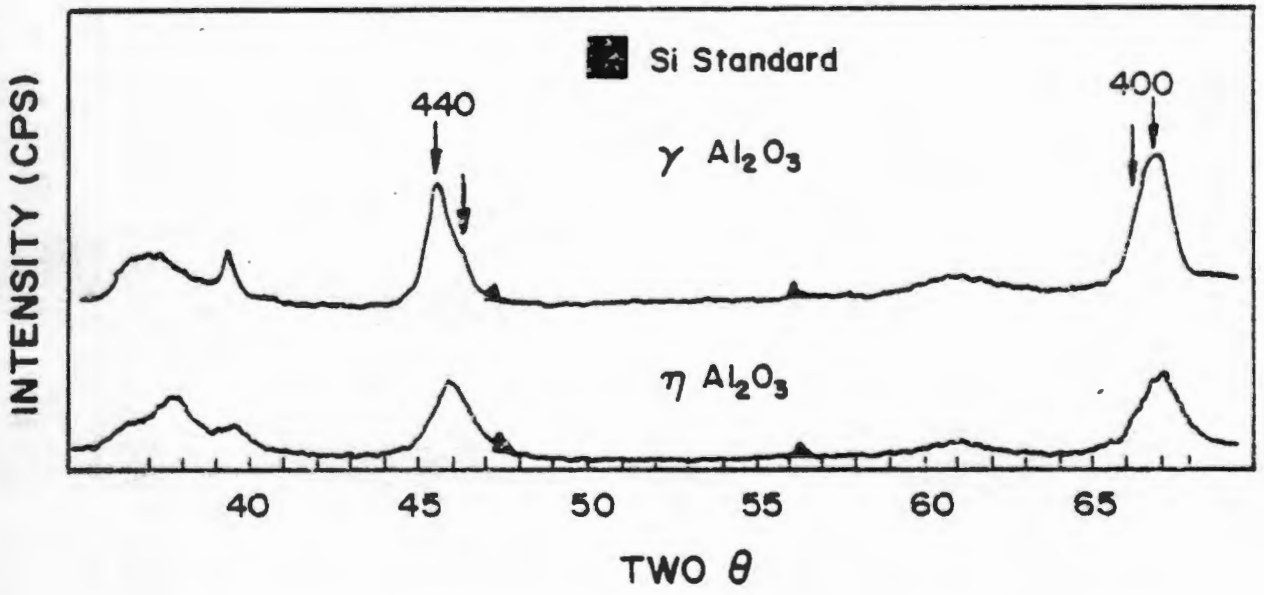

FIGURE 4.11: Comparative XRD trace of γ-Al_2O_3 and η-Al_2O_3 indicating tetragonal distortion

Apart from the occupation of the octahedral sites, γ- and η-Al_2O_3 are very similar. Significantly, both compounds have an [...ABC ABC...] oxygen sublattice which is maintained intact until the shear transformation to α-Al_2O_3, which occurs at about 1200 °C.

A $(11\bar{2}0)$ section through the idealized structure of β''-Al_2O_3 (Fig. 4.12) shows that the compound consists of spinel blocks containing oxygen ions in the close-packed cubic arrangement. X-ray intensity calculations by Whittingham and Huggins (1971) supported by work of Le Cars et al. (1972) suggested that the most likely arrangement of the oxygen is as follows:

[...ABCABCABCABCABCABCAB...]

The underlined oxygen ion layer represents the conduction plane, which contains a third of the oxygen ions of the close-packed layers. The similarity in the stacking order of the oxygen sublattice of γ-and η-Al_2O_3 with the β"-Al_2O_3 oxygen sublattice suggests a possible mechanism by which β"-Al_2O_3 is formed directly from these transition aluminas when lithium and sodium salts are present.

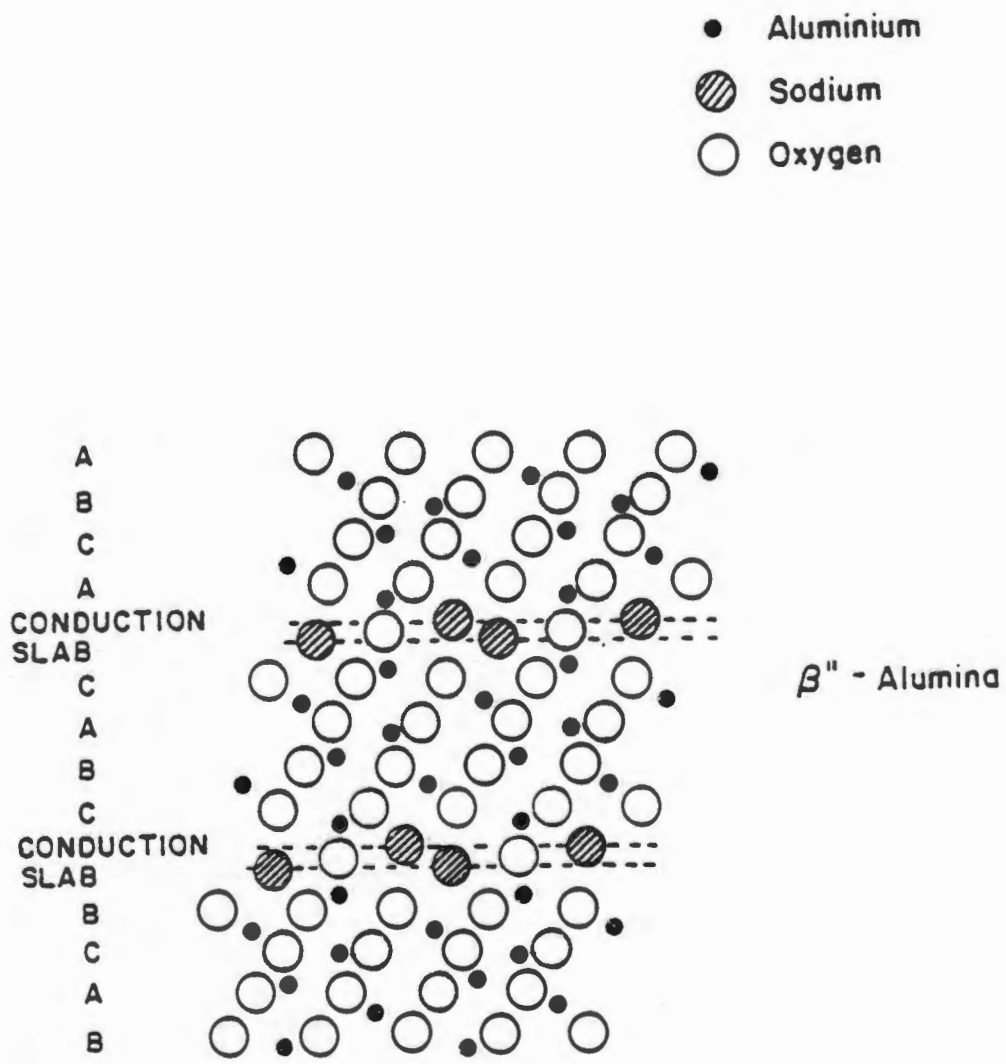

FIGURE 4.12: A $(1\bar{1}20)$ section through the idealized structure of β"-Al_2O_3

After the dehydroxylation of boehmite or bayerite, lithium diffuses through a three-dimensional network of face-shared tetrahedra and octahedra of the close-packed cubic oxygen lattice of the γ- and η-alumina structures and ion exchanges with the residual hydrogen ions. The lithium ions stabilize the close-packed cubic oxygen sublattice. It has been demonstrated by DTA that small amounts of lithium (~2 mol percent) considerably increase the transformation temperature of the transition alumina to α-Al_2O_3. This increase in transformation temperature can be ascribed to the formation of a lithium-stabilized, close-packed cubic transition alumina. In the proposed mechanism, the function of the lithium is to 'pin' the cubic oxygen sublattice, which is formed upon dehydroxylation. The sodium ions, which are larger than the oxygen ions, are not accommodated in the crystal lattice at low temperatures. It is suggested that the sodium ions reside on the surface of the transition alumina grains as an amorphous soda phase until a temperature is reached which makes it thermodynamically feasible for the sodium to diffuse into the oxygen sublattice to form the β''-Al_2O_3 conduction layers.

When lithium is absent from the reaction mixture, the crystallization pathway is substantially different and the reaction product at 1200 °C contains α-Al_2O_3, γ-$NaAlO_2$, β''-Al_2O_3 and β-Al_2O_3. Consistent with the previous observations, the dehydroxylation of bayerite and boehmite produces η- and γ-alumina respectively. When only sodium is present, two simultaneous reactions take place during the heating of the reaction mixture. A portion of the transition alumina transforms to α-Al_2O_3 as no lithium is present to stabilize the close-packed cubic oxygen sublattice. The rest of the transition alumina proceeds to an unstabilized β''-Al_2O_3 by the reaction of sodium with the material. The α-Al_2O_3 reacts with the sodium to form β- and β''-Al_2O_3 mixtures via γ-$NaAlO_2$ intermediate.

At 1600 °C, the reaction product of boehmite and soda is similar to that of a material derived from the α-Al_2O_3 precursor.

The reaction products of the materials derived from boehmite and bayerite in the absence of the lithium, demonstrate that two important criteria must be satisfied to allow pure β"-Al_2O_3 to be formed. Firstly, a regular close-packed cubic oxygen sublattice must be formed upon dehydroxylation of the hydroxide material and secondly the sublattice must be maintained or stabilized to prevent the transformation to α-Al_2O_3 before the reaction with soda can occur.

4.3.3 Intergrown β/β"-Al_2O_3 Polytypes

Disordered pseudoboehmite and gibbsite produced a reaction product which was broadly classified as an intergrown β/β"-Al_2O_3 polytype. This material is characterized by the simultaneous presence of broad and sharp XRD peaks as discussed in Sections 2.5 and 4.2.3.

Poulieff et al. (1978) and Morgan (1976) reported these materials and suggested that they were formed from disordered precursors. According to Poulieff et al. (1978) intergrown β/β"-Al_2O_3 was formed as a consequence of the retention of the precursor stacking faults. Hodge (1983) postulated the epitaxial nucleation of β and β"-Al_2O_3 on the disordered substrate followed by the subsequent growth of the phases. In none of the above cases, was the role of the lithium or an initial close-packed cubic oxide lattice alluded to.

The formation of the intergrown phases can be explained by a modification of the model of Poulieff et al. (1978). It has been demonstrated that both pseudoboehmite and gibbsite dehydroxylate to poorly ordered transition alumina phases. Pseudoboehmite produces a virtually amorphous transition

alumina product while gibbsite produces poorly ordered χ-Al_2O_3 after dehydroxylation. The highly mobile lithium ions diffuse into the structure after dehydroxylation, exchange for the hydrogen ions and stabilize the faulted cubic oxygen sublattice. As in the case of the γ- and η- Al_2O_3, sodium is accommodated on the surface of the grain. Because of the higher density of faults and irregularities in the transition alumina derived from pseudoboehmite and gibbsite, sodium diffuses into the structure at lower temperatures to form beta alumina polytypes, which retain the original disordered oxygen sublattice. The disordered sublattice is partially maintained by lithium occupation of tetrahedral and octahedral sites. The disordered β/β''-Al_2O_3 polytypes are very stable once formed and the structures are retained even at 1600 °C.

When pseudoboehmite and gibbsite are reacted with sodium in the absence of lithium, a different reaction product and crystallization mechanism is observed. With no lithium present to maintain the cubic oxygen sublattice, the disordered transition alumina converts to α-Al_2O_3. The α-Al_2O_3 reacts with soda to form a distinctly two-phase mixture of β and β''-Al_2O_3 via a sodium aluminate intermediate. As in the case of boehmite and bayerite, the 1 600 °C product of pseudoboehmite and gibbsite in the absence of lithium resembles that of an α-Al_2O_3 derived material.

4.4 CONCLUSIONS

On the basis of the three observed crystallization pathways, a generalized mechanism for the formation of beta alumina compounds from aluminium hydroxides and soda and lithia is proposed. Dehydroxylation of aluminium hydroxides produce cubic oxygen sublattices with a variety of oxygen stacking sequences. Three distinct classes of sublattices were reported by Krishner (1971): An α-series with [...AB AB...] stacking order (e.g. diaspore), a β-series with [...ABAC ABAC...] stacking order (e.g. gibbsite) and a γ-series with [...ABC ABC...] stacking order (e.g. boehmite, bayerite, nordstrandite). Collectively these materials are referred to as transition aluminas and are stabilized by the presence of hydrogen ions. It is suggested that lithium ions diffuse into the oxygen sublattice of the transition alumina and replace the hydrogen ions by ion exchange. The lithium ions pin the original oxygen sublattice and prevent the transformation to α-Al_2O_3 as the temperature is increased. The sodium ions are associated with the surface of the aluminium oxide grain in an amorphous soda phase. When a sufficiently high temperature is reached, the sodium diffuses into the grains along regions of structural weakness, e.g. strain, stacking faults and dislocations etc. to form a conduction layer. Little rearrangement of the oxygen sublattice is observed which implies that the nature of the beta alumina product is critically dependent on the nature of the ordering of the precursor sublattice.

CHAPTER 5

CONCLUSIONS AND FUTURE RESEARCH AREAS

This thesis has reported the synthesis and characterization of a range of aluminium hydroxide materials from a common aluminium isopropoxide parent material. These synthetic aluminium hydroxides were used to produce a range of beta alumina powders by the solid state reaction with sodium and lithium carbonates. The solid state reactions were carried out over a wide temperature range and the reaction products were characterized by DTA and XRD methods.

A qualitative mechanism for the formation of beta alumina powders from aluminium hydroxide precursors is proposed. Dehydroxylation of aluminium hydroxide precursors produce three distinct cubic oxygen sublattice types with different oxygen stacking sequences. These reordering sequences are called transition aluminas and are stabilized by the presence of hydrogen ions. It is suggested that the lithium stabilizer ions diffuse into the transition alumina matrix and replace the hydrogen ions by ion exchange. The lithium ions 'pin' the original oxygen sublattice and prevent the transformation to α-Al_2O_3 as the temperature is increased. The relatively large sodium ions are associated with the surface of the aluminium oxide grain in an amorphous phase. When a sufficiently high temperature is reached, the sodium ions diffuse into the grains to form β''-Al_2O_3.

Little rearrangement of the oxygen sublattice is thus required which implies that the nature of the beta alumina product is dependent on the order of the precursor sublattice.

Pure β''-Al_2O_3 is formed when lithium ions are exchanged for hydrogen ions in a transition alumina matrix with an γ-oxygen sublattice [...ABC ABC...] followed by the reaction of this species with sodium ions.

An intergrown β/β''-Al_2O_3 polytype results from the reaction of sodium ions with either a disordered transition alumina matrix or β-oxygen sublattice [...ABAC ABAC...] in which the hydrogen ions have been exchanged by lithium ions.

Distinct two-phase β- and β''-Al_2O_3 results from the reconstructive transformation of either an α-oxygen sublattice [AB AB] or by the reaction of sodium with unstabilized aluminium hydroxide materials.

The conclusions have an important impact on the raw material selection for the production of β''-Al_2O_3 ceramic tubes. Hydrothermal boehmite of sufficient purity is a cheaper raw material than high purity α-Al_2O_3 and would reduce the production costs substantially.

Results from this thesis suggest further research in the following areas:

Pure β''-Al_2O_3 is formed when an ordered oxygen sublattice is reacted with lithium and sodium salts. Further investigations of aluminium-containing precursors producing a well-ordered oxygen sublattice must be carried out. The degree of order in the sublattice needs to be quantified and related to the ability of the materials to produce only β''-Al_2O_3 when reacted with soda and lithia carbonates.

Transition aluminas are known to produce poor X-ray diffraction spectra which makes it difficult to establish the exact crystallographic relationships between the transition aluminas and the beta alumina reaction products. The arguments in this thesis were based on the nature of the oxygen sublattice and the role of lithium. Techniques need to be established which would enable the establishment of the crystallographic relationships between the transition aluminas and the final beta alumina products. For example, low kV TEM techniques may have some promise although initial work has shown problems in the thinning of powdered samples.

REFERENCES

Abrams, L and Louw, M J D, Ind. Eng. Chem. Product R&D, **8**, 38 (1969).

Barrow, P, Duncan, J H, Van Zyl, A and Kingon, A I, UK patent 8612645 (1986).

Barrow, P, Technical note No. 4, Beta R&D, Derby (1986).

Beevers, C A and Brohult, S, Z. Kristallogr., **95**, 472-474 (1936).

Bevan, D J, Hutson, B and Mosely, P T, Mat. Res. Bull., **9**, 1073 (1974).

Bradley, D C, Mehrotra, R C, Guar, D P, Metal Alkoxides, Academic Press, London, 1978.

Bragg, W L, Gottfied, G and West, J, Z. Kristallogr., **77**, 255-274 (1931).

Bugden, W G and Duncan, J H, Institute of Metallurgists Conference on Phase Transformations, York, April 1979, Series 3, 11 (2) (11-12)

Byckalo, W, Rosenblatt, G, Lam, J and Nicholson, P S, Am. Ceram. Soc. Bull., **55**, 286 (1976).

Bye, G C and Robinson, J G, Kolloid-Z., Z. Polym., **198**, 53-60 (1964).

Chandry, V and Cannon, R M, Mater. Sci. Res., **11**, 443 (1978).

Coetzer, J, J. Power Sources, **18**, 337-380 (1986).

Conradi Vic Mr - Personal communication (1986).

De Jonge, L C, J. Mat. Sci., **12**, 497-502 (1977).

De Vries, R C and Roth, W L, J. Am. Ceram. Soc., **52(7)**, 364-369 (1969).

Deplanches, G, 4th DOE/EPR/Sodium Sulphur Battery Workshop, Marcoussis (1980).

Duncan, G K and West, A R, Solid State Ionics, **9/10**, 259 (1983).

Duncan, G K, PhD Thesis, Aberdeen, 1985.

Duncan, J H and Bugden, W G, Special Ceramics, **7**, 221 (1981).

Duncan, J H, British Patent 83/335641 (1983).

Duncan, J H, Solid electrolyte production, in The Sodium Sulphur Battery, (eds J Sudworth & R Tilley) Chapman Hall, London, 1985.

Elliot, A G and Huggins, R A, J. Am. Ceram. Soc., **58** [11-12], 497-500 (1975).

Ervin, G and Osborn, E F, J. Geol., **59**, 381-94 (1951).

Ewing, F J, J. Chem. Phys., **3**, 203-7 (1935).

Eyrand, C, Acad. Sci., **240**, 862-4 (1965).

Fally, J, Lasne, C, Lazennec, Y and Margotin, P, J. Electrochem. soc., **120**, 1296 (1973).

Feinknecht, W, Wittenbach, A and Buser, W, 4th Symp. Reactiv. Solids, Elsevier, 234-9 (1961).

Freund, F, Ber. Deut. Keram. Ges., **44**, 141-7 (1967).

Fricke, R and Jockers, K, Z. Naturforsch., **2b**, 244 (1947).

Fricke, R and Schmäh, H, Z. Anorg. Chem.. **255**, 253-68 (1948).

Fricke, R and Wullhorst, B, Z. Anorg. Allg. Chem., **205**, 127-44 (1932).

Ginsberg, H and Köster, M, Z. Anorg. Chem., **271**, 41-8 (1952).

Ginsberg, H, Hüttig, W and Stehl, H, Z. Anorg. Allg. Chem., **309**, 233-44 (1961).

Ginsberg, H, Hüttig, W and Stiehl, H, Z. Anorg. Allg. Chem., **318**, 238-56 (1962).

Ginsberg, H, Hüttig, W and Strunk-Lichtenberg, G, Z. Anorg. Allg. Chem., **293**, 33-46, 204-13 (1957).

Gordon, R S , NSF Tech. Report Contract NO NSF C805 (1976).

Goton, R, Thesis, No. 146, Univ. Lyon, 9 July 1955.

Green, D J and Hutchinson, S, Mat. Sci. Mong., **6**, 964 (1980).

Hauschild, U, Brit. Patent 950,165 (1964a).

Hauschild, U, Ger. Patent 1,182,643 (1964b).

Hauschild, U, Z. Anorg. Allg. Chem., **324**, 15-20 (1963).

Highe, A J, PhD Thesis, California Institute of Technology (1981).

Hodge, J D, Am. Ceram. Soc. Bull., **62** [2], 244-248 (1983).

Johnson, D W, Granstaff, S M and Rhodes, W W, Am. Ceram. Soc. Bull., **58(9)**, 849-52 (1979).

Jorgensen, J.D., Solid State Ionics, **5**, 143 (1981).

Kennedy, G C, Amer. J. Sci., **257**, 563-73 (1959).

Kraut, H, Flake, E, Schmidt, W and Volmer, H, Ber., **57B**, 1357-73 (1942).

Krishner, H, Trav. Com. Int. Etudes Bauxite, Oxides, Hydroxides Alum., **7**, 107-16 (1971).

Laubengayer, A W and Weiss, R S, J. Amer. Chem. Soc., **65**, 247-50 (1943).

Le Cars, Y, Théry, J and Collongues, R, Rev. Hautes Temp. Refract., **9(1)**, 153-160 (1973).

Le Cars, Y, Théry, J and Collougues, R, Rev. Int. Hautes, Temp. Refract., **9**, 513 (1972).

Lippens, B C, Thesis, Delft (1961).

Manan, G D, International Conf. on Superionic Conductors, Schenectady NY, 115-134 (1976).

Marboe, E C and Bentur, S, Silicates Ind., **26**, 389-399 (1961).

May, G J, J. Power Sources, **3**, 1 (1978).

Megaw, H D, Z. Kristallogr., **A87**, 185-204 (1934).

Milligan, W O and McAtee, J L, J. Phys. Chem., **60**, 273-7 (1956).

Morgan, P E D, Mat. Res. Bull., **11**, 283 (1976).

Mosely, P T, The solid electrolyte properties and characteristics, Chapter 2 from the Sodium Sulphur Battery, (eds J L Sudworth & A R Tilley) Chapman and Hall, London 1985.

Neuhaus, A and Heide, H, Ber. Deut. Keram. Ges., **42**, 167-84 (1975).

Papée, D, Tertian, R and Biais, R, Bull. Soc. Chim. Fr., 1301-10 (1958).

Pauling, L, The nature of the chemical bond, 3rd Ed., Cornell University Press (1963).

Pekarsky, A and Nicholson, P S, Mat. Sci. Res., **15**, 1517 (1980).

Peters, C R, Bettman, M, Moore, J and Glick, M, Acta Cryst., **B27**, 1826 (1971).

Pett, R A, Runkle, F D, Tennhouse, G J and Theodore, A N, Am. Ceram. Soc. Bull., **61**, 992 (1982).

Petz, J I, J. Chem. Phys., **48**, 901-11 (1968).

Poulieff, K N, Kvackkov, R and Balkonor, I M, Mat. Res. Bull., **13**, 323 (1978).

Powers, R W, J. Electrochem. Soc., **122**, 490 (1975).

Rankin, G A and Merwin, H E, J. Amer. Chem. Soc., **38**, 568-588 (1916).

Reichartz, P D and Fost, W J, J. Chem. Phys., **14**, 495 (1946).

Roth, W L, Superionic conductors (eds. G D Mahon & W L Roth) Plenum Press, 223 (1976).

Rothbauer, R, Zigan, F and O'Daniel, H, Z. Kristallogr., **125**, 317-31 (1967).

Saalfeld, H and Jarchow, O, Neues, Jahrb. Mineral. Abh., **109**, 185-91 (1968).

Saalfeld, H, Neues, Jahrb. Mineral. Abh., **95**, 1-87 (1960).

Sato, T, J. Appl. Chem., **12**, 9-12 (1962).

Schmäh, H, Z. Naturforscher, **1**, 323-4 (1946).

Scholder, R and Marsmann, M, Z. Anorg. Allg. Chem., **321**, 246-261 (1963).

Souza Santos, P, Vallejo-Freire, A and Souza Santos, H L, Kolloid-Z., **133**, 101-7 (1953).

Stumpf, H C, Ind. Eng. Chem., **42**, 1398-1403 (1950).

Sudworth, J L, Proc. 10th Intersoc. Energy Conv. Eng. Conf., NY, 624 (1975).

Takahashi, T and Kuwabara, K, J. Appl. Electrochem., **10**, 291-297 (1980).

Tan, S R and May, G J, Science of Ceramics, **9**, (ed. K J de Vries) 103 (1977).

Teichner, S, C. R. Acad. Sci., **237**, 810-2 (1953).

Tertian, R and Papée, D, J. Chim. Phys., **55**, 341-53 (1958).

Torkar, K and Bergmann, O, Monatsh. Chem., **91**, 400-5 (1960).

Torkar, K and Egghart, H, Monatsh. Chem., **92**, 755-67 (1961).

Unmack, A, 2nd Int. Congr. Crystallogr. Abstr. of Papers, Stockholm, June 27 to July 5, 1951 (Inorganic Structures No. 8 Section G).

Van Nordstrand, R A, Hettinger, W P and Keith, C D, Nature, **177**, 713-4 (1956).

Van Zyl, A, Kingon, A I and Smit, P M, NIMR/CSIR Report CMAT 192, (1985a).

Van Zyl, A and Kingon, A I, NIMR/CSIR Report CMAT 241, (1985b).

Van Zyl, A, Kingon, A I, and Smit, P M, Mat. Sci. and Eng.-**78**, 217-222 (1985b).

Van Zyl, A and Duncan, G K, NIMR/CSIR Report CMAT 312 (1986a).

Van Zyl, A and Duncan, G K, NIMR/CSIR Report CMAT 313 (1986b).

Vikar, A V, Miller, M L, butler, I B and Gordon, R S, US Patent 4 113 928 (1978).

Vogel, E M, Johnson, D W and Yan, M F, Am. Ceram. Soc. Bull., **60(4)**, 494-96 (1981).

Wang, J C, J. Chem. Phys., **63**, 772 (1975).

Watson, J H L, Vallejo-Freire, A, Souza Santos, P and Parsons, J, Kolloid-Z., **154**, 4-15 (1957).

Weber, N and Venero, A F, Abstracted in Am. Ceram. Soc. Bull., **49(4)**, 491 (1970).

Wefers, K, Erzmetall., **18**, 459-63 (1965).

Wefers, K, Metall., **21**, 423-31 (1967).

Weiser, H B and Milligan, W O J, Phys. Chem., **38**, 1175-82 (1934), 1.

West, A, Mater. Res. Bull., **14**, 44i (1979).

Whittingham, M S and Huggins, R A, J. Chem. Phys., **54**, 414 (1971).

Willstütter, R, Kraut, H and Erbacher, O, Ber., **58B**, 2448-58 (1925).

Yoldas, B E, J. Appl. Chem. Biotechnol., **23**, 803-809 (1973).

Yoldas, B E and Partlow, D P, Am. Ceram. Soc. Bull., **55(6)**, 640-42 (1980).

Youngblood, G E, Vikar, A V, Cannon W R and Gordon R S, Am. Ceram. Soc. Bull., **56**, 206 (1977).